Спектроскопия комбинационного рассеяния
&
SERS - Surface-enhanced Raman scattering

Калмыков Алексей

Raman scattering

Non resonant Raman Scattering

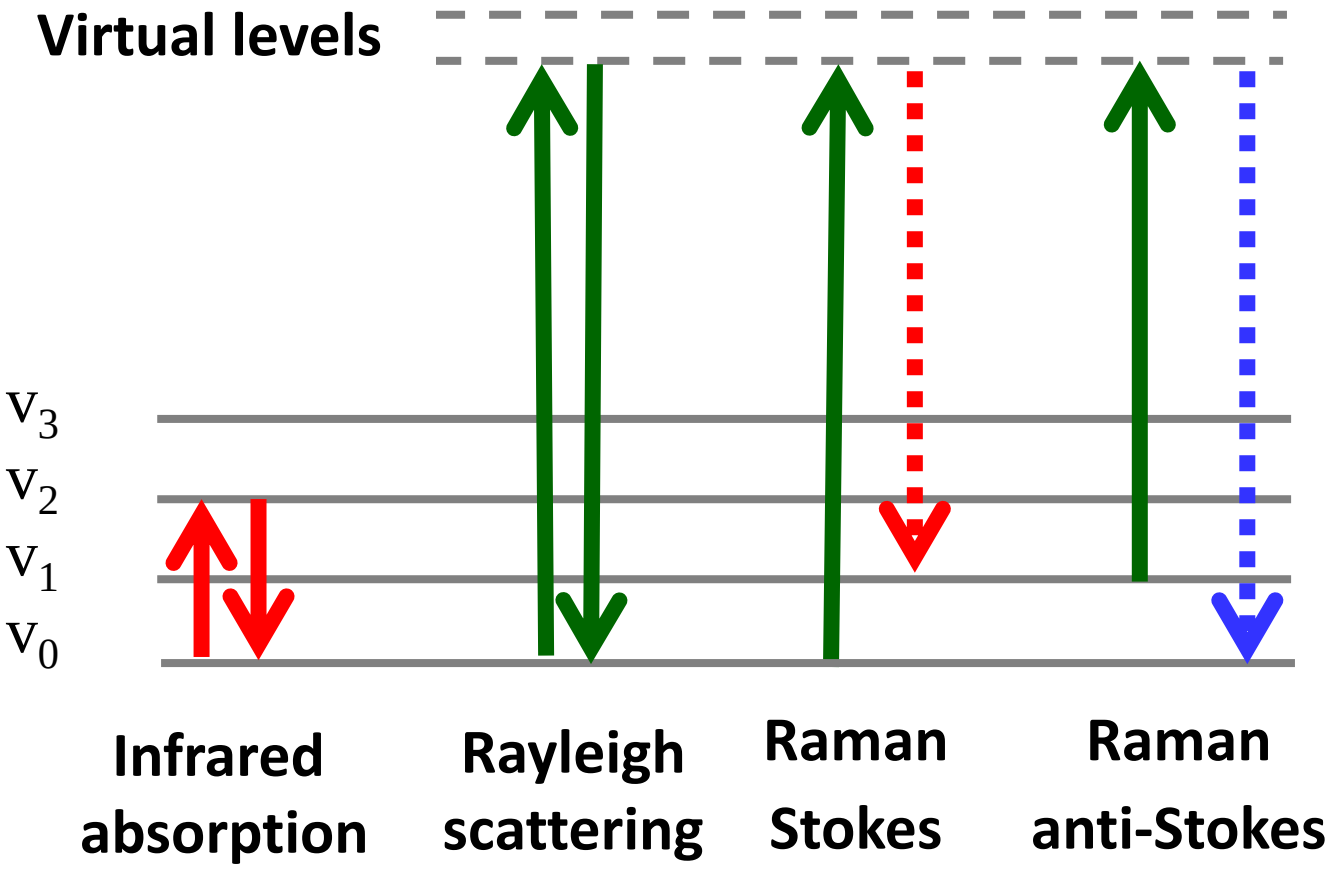

$$I_{NRS}(\nu_S) = N\, I(\nu_L)\, \sigma_{R,free}$$

σ ~ 1E-30

Raman`s setup

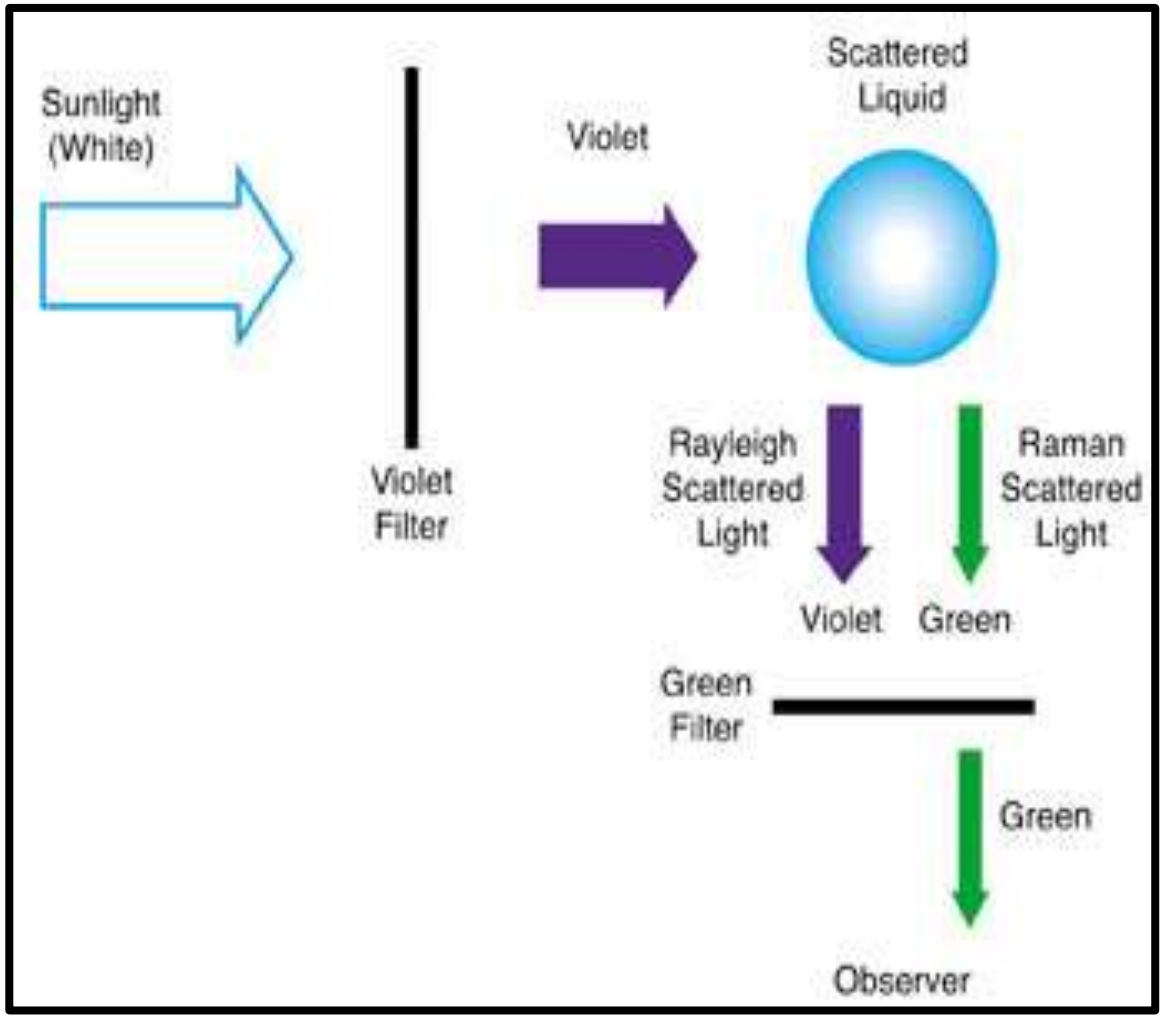

Raman visible through unaided eye

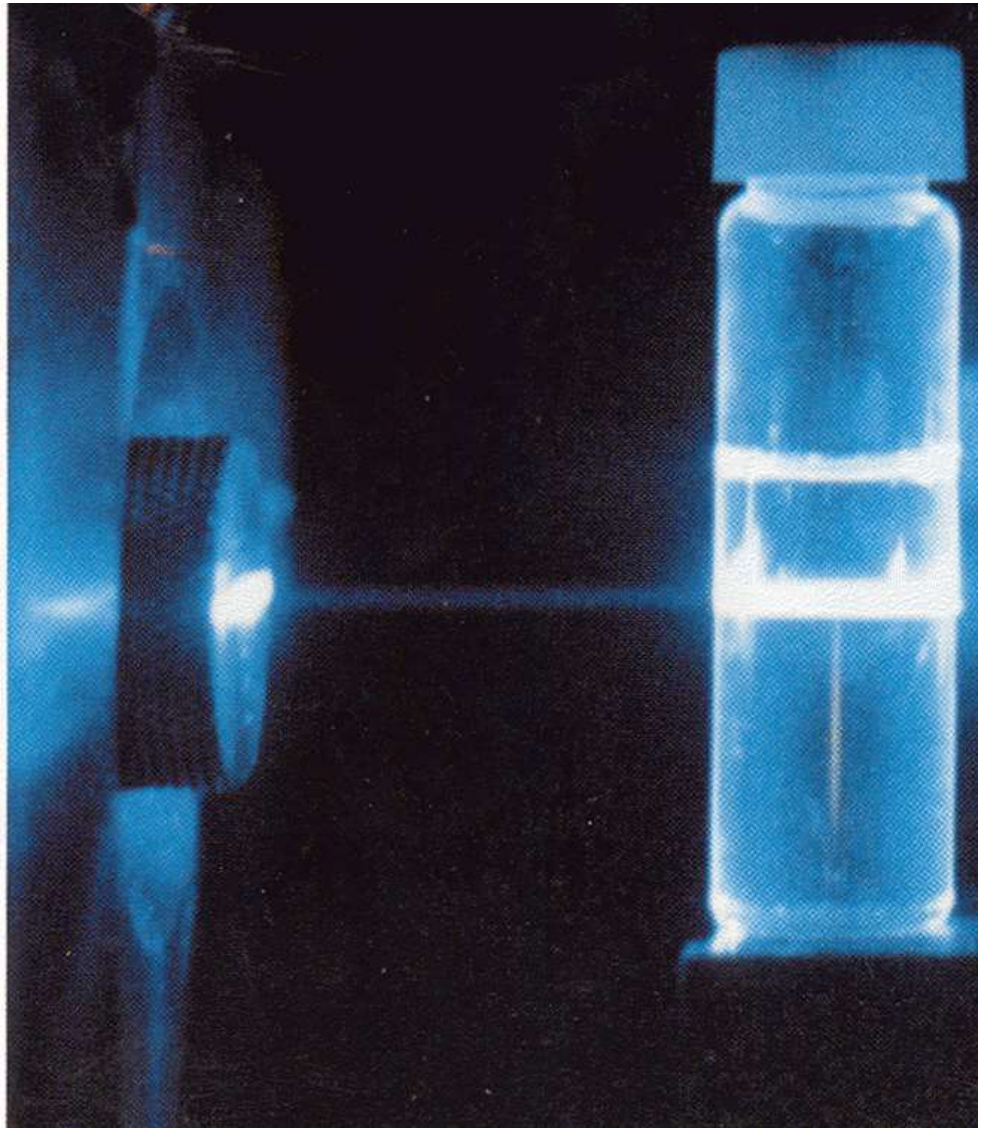

Raman scattering history

- В 1918 г. Л. И. Мандельштам предсказал расщепление линии рэлеевского рассеяния вследствие рассеяния света на тепловых акустических волнах
- в 1923 году независимо от Мандельштама Смекал теоретически предсказал явление неупругого рассеяния.
- Впоследствии 21 февраля 1928 г. Ландсберг и Мандельштам обнаружили эффект комбинационного рассеяния света в кристаллах
- 1928 год Ч. В. Раман и его студент К. С. Кришнану обнаружили линии спектра нового излучения в экспериментах по рассеянию света в жидкостях и парах.
- 1961 – изобретение лазера
- 1977 – SERS
- 1997 – single molecule SERS

Raman scattering (theory)

$E = E_0 \cos 2\pi\omega_l t$ *incident electromagnetic wave (laser beam)*

$P = \alpha E = \alpha E_0 \cos 2\pi\omega_l t$ *induced electric dipole moment ;* $\boldsymbol{\alpha}$ *is the polarizability*

$$I = \frac{16\pi^4}{3c^3} \nu_l{}^4 P^4$$ *classical expression of total scattered light*

$$\alpha = \alpha_o + \left(\frac{\delta\alpha}{\delta Q_k}\right)_0 Q_k + \cdots$$ $\boldsymbol{\alpha}$ *is polarizability that changes by molecular vibration;* $\boldsymbol{Q}$ *is coordinate that describes molecular vibration*

Rayleigh scattering — Anti-Stokes Raman scattering — Stokes Raman scattering

$$P = \alpha E = \alpha_o E_0 \cos 2\pi\omega_l t + \frac{1}{2} E_0 Q_k{}^0 \left(\frac{\delta\alpha}{\delta Q_k}\right)_0 [\cos 2\pi(\omega_l + \Omega)t + \cos 2\pi(\omega_l - \Omega)t]$$

Intensity Values at ~ 1500 cm^{-1}

$I(\omega_l) >> I_S >> I_{aS}$

$1 >> 10^{-7} >> 10^{-9}$

$$\frac{N_1}{N_0} = e^{-\frac{h\nu_{vib}}{kT}}$$

~1E2

Raman scattering (theory)

Polarizability ellipsoids of CO2 molecule.

$$\frac{\delta\alpha}{\delta Q_k} \neq 0$$

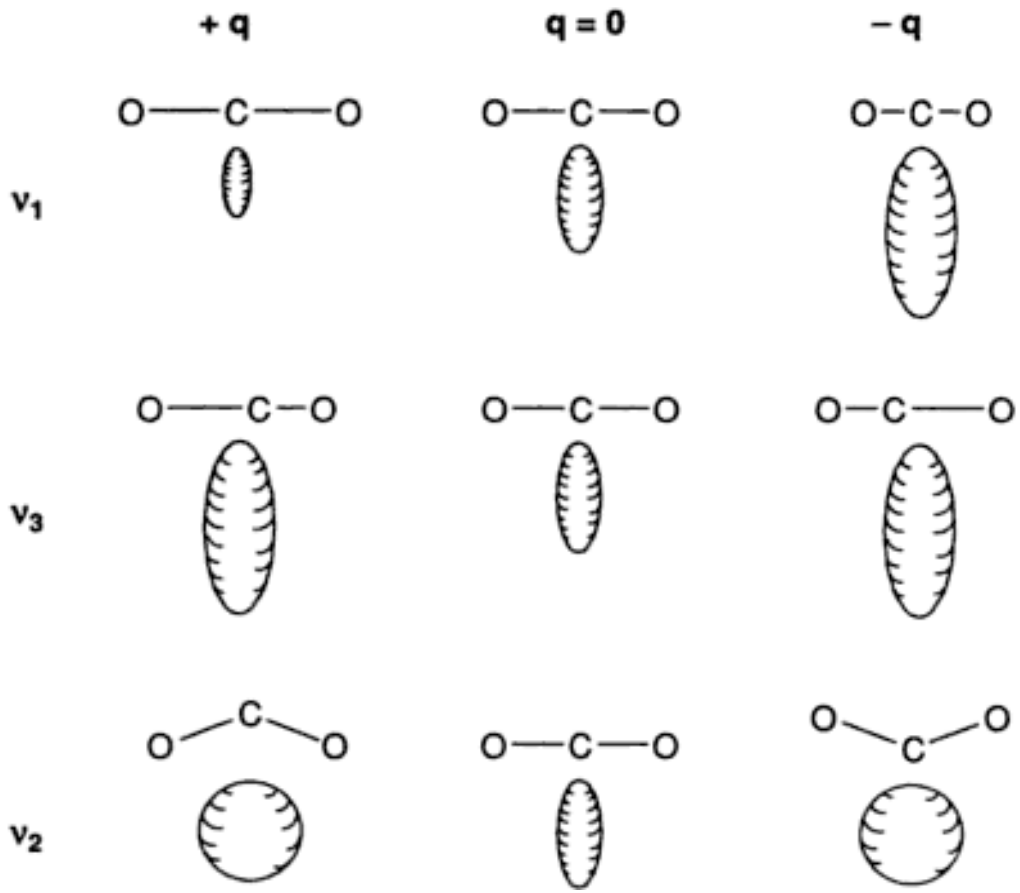

IR inactive Raman active

IR active Raman inactive

Information from Raman spectroscopy

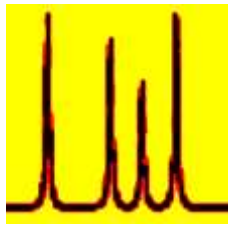

Characteristic Raman frequencies → What is this?

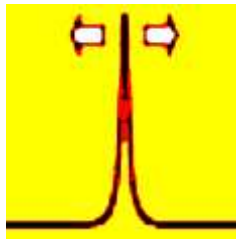

Changes in frequency of Raman peak → Chemical interaction; stress; strain; temperature

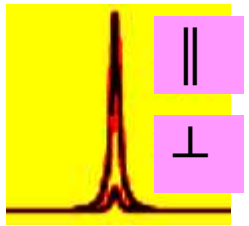

Polarization of Raman peak → Crystal symmetry ; orientation;

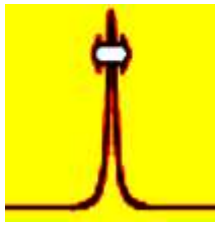

Width of Raman peak → Morphology

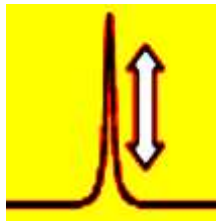

Intensity of Raman peak →

- Amount of material; film thickness;
- Nonlinear optical effects

Methods of amplification of the Raman emission

- **Resonant Raman Scattering**

~1E3-1E4

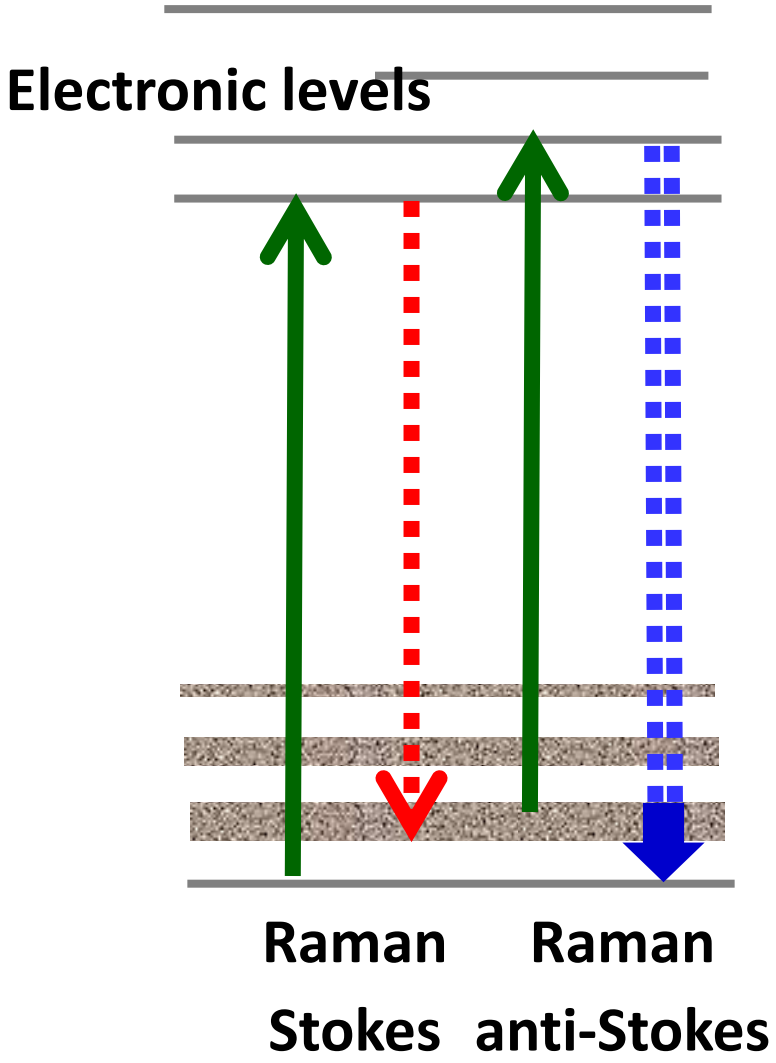

- **Surface-Enhanced Raman Scattering**

~1E5-1E9

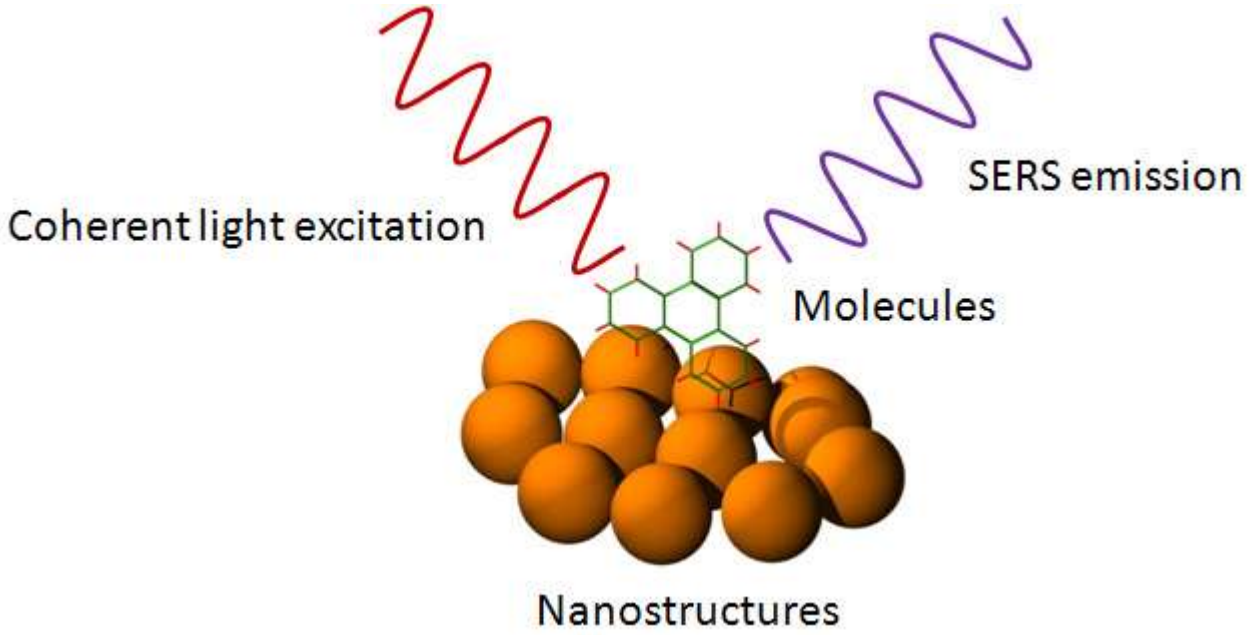

- **Stimulated Raman Scattering**
- **Coherent anti-Stokes Raman**

Stimulated Raman Scattering

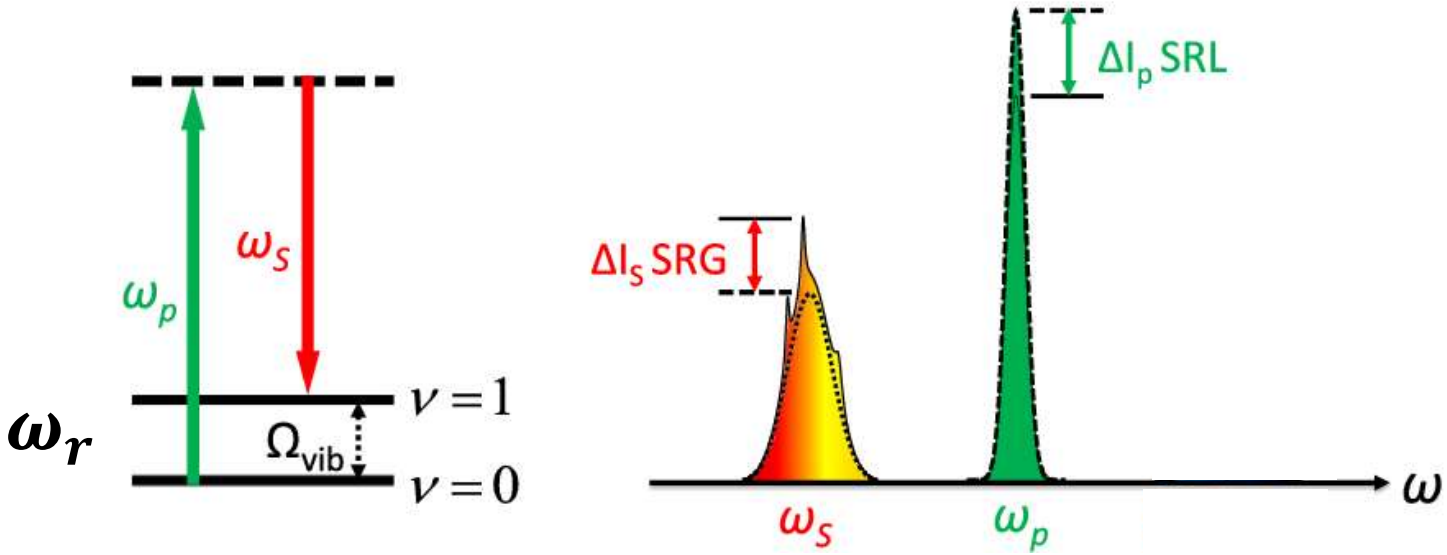

$$\omega_r = \omega_p - \omega_s$$

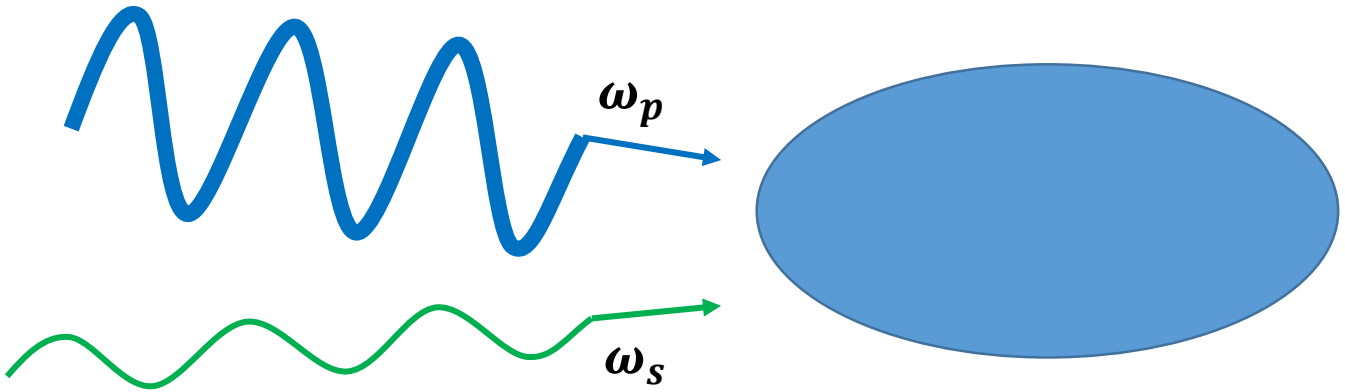

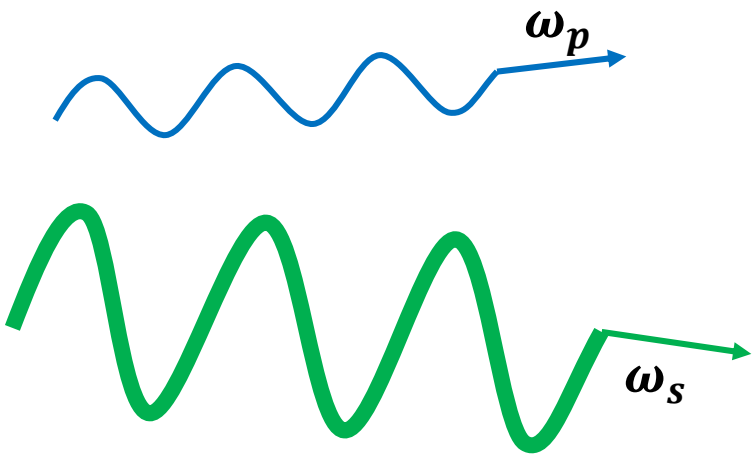

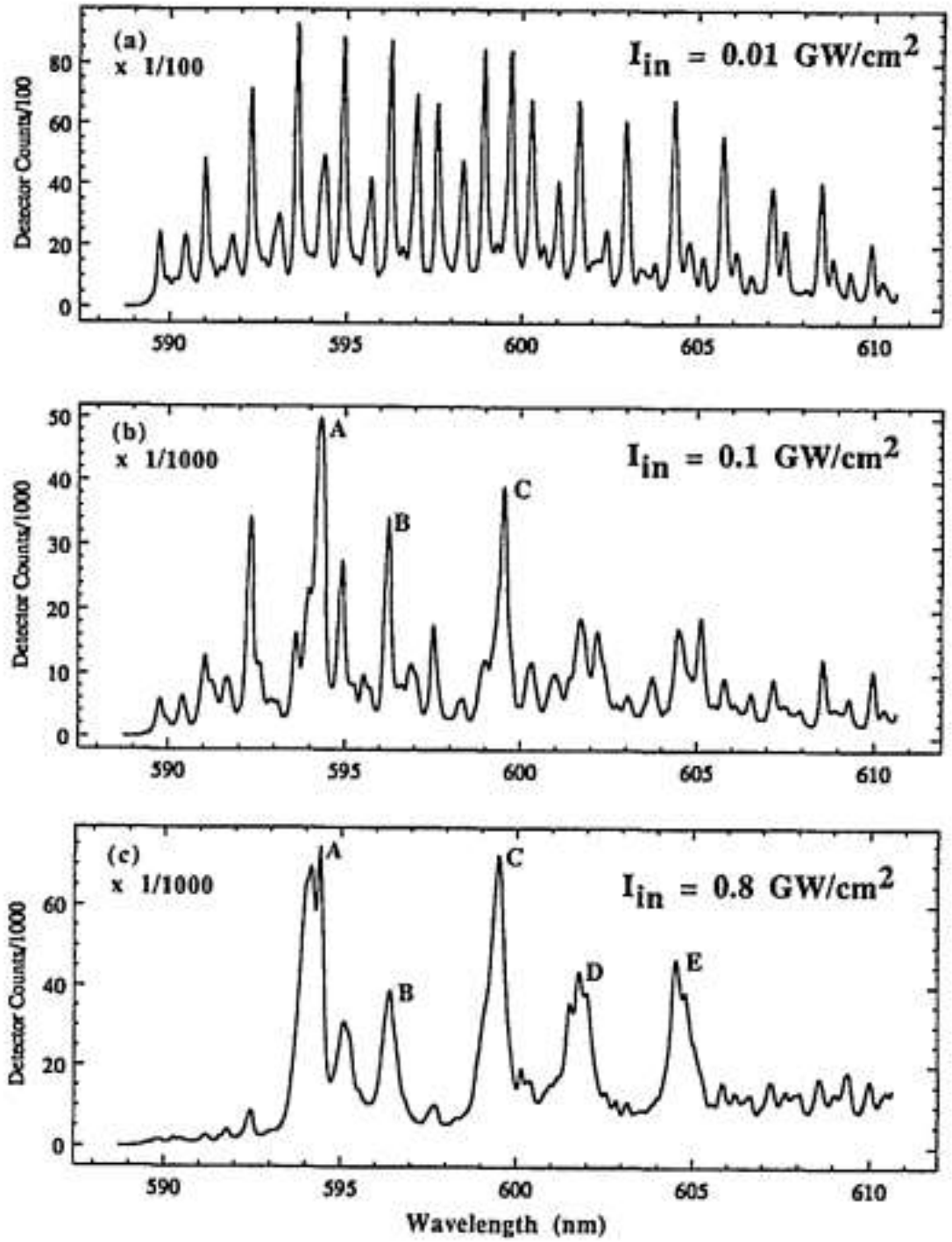

Stimulated resonance Raman scattering of Rhodamine 6G

A microdroplet (typically of 10-50,um radius) acts as a broadband dielectric cavity.
10^{-3} M R6G λ= 550 nm.

A, B, C, D and E with Stokes shifts of 1361, 1415, 1507, 1569 and 1645 cm^{-1}

Kwok A. S., Chang R. K. Stimulated resonance Raman scattering of Rhodamine 6G //Optics letters. – 1993. – Т. 18. – №. 20. – С. 1703-1705.

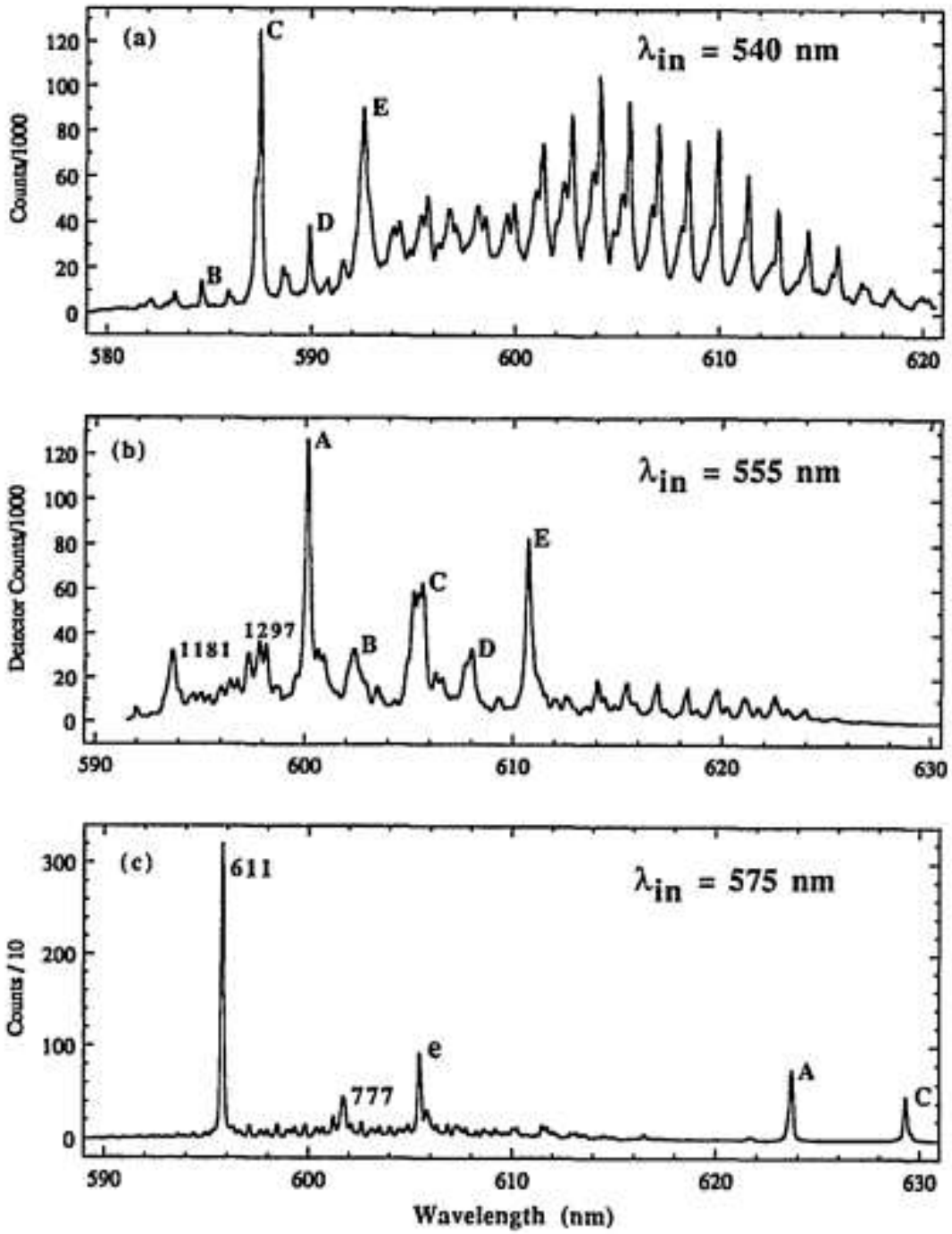

SRRS and lasing from 10^{-3} M R6G in ethanol droplets irradiated with I = 0.8 GW/cm^2

$$I_C(\lambda=540\text{ nm})/I_C(\lambda=575\text{ nm}) \sim \mathbf{250}$$

Kwok A. S., Chang R. K. Stimulated resonance Raman scattering of Rhodamine 6G //Optics letters. – 1993. – Т. 18. – №. 20. – С. 1703-1705.

Surface-Enhanced Raman Scattering

Electromagnetic Enhancement

a nanosphere $\mathbf{E}_{\mathbf{surface}} = \dfrac{3\varepsilon}{\varepsilon + 2\varepsilon_m}\mathbf{E}_0$

ε metal dielectric function

ε_m medium dielectric function

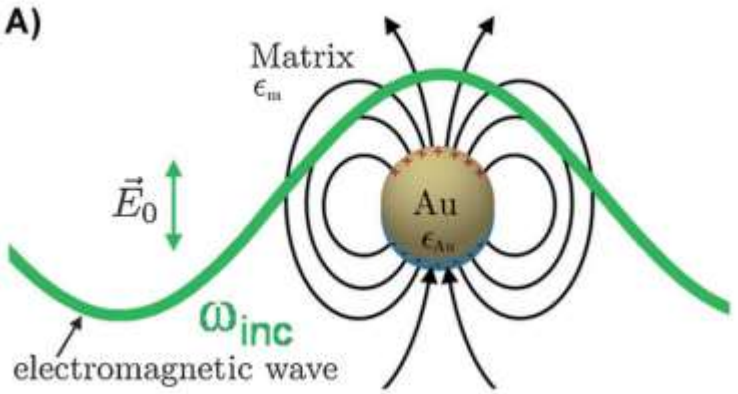

$$^{em}G_{SERS}(r_m, \nu) = \left| \frac{E(r_m, \nu)}{E_{inc}(\nu)} \right|^4$$

(1) E.m. field enhancement

max. ~ 10^6 (isolated Ag,Au)

max. ~ 10^8 (coupled)

The 'Chemical' (Charge Transfer) Mechanism

A new charge transfer band is formed when a molecule is adsorbed on a metal surface

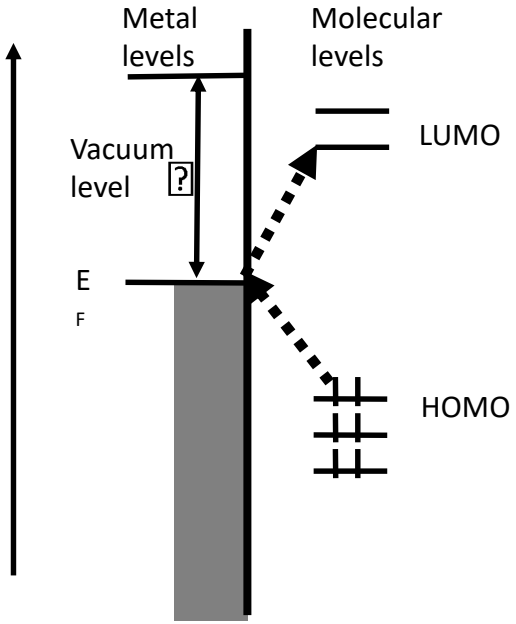

(2) Chemical enhancement

max. 10-100

Plasmonic nanogap-enhanced Raman scattering

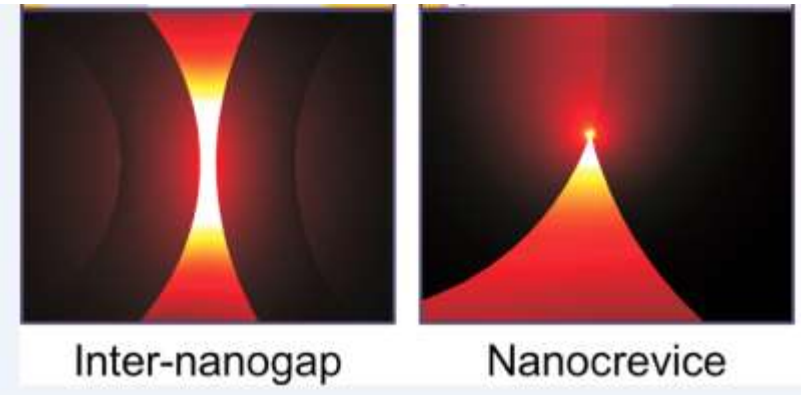

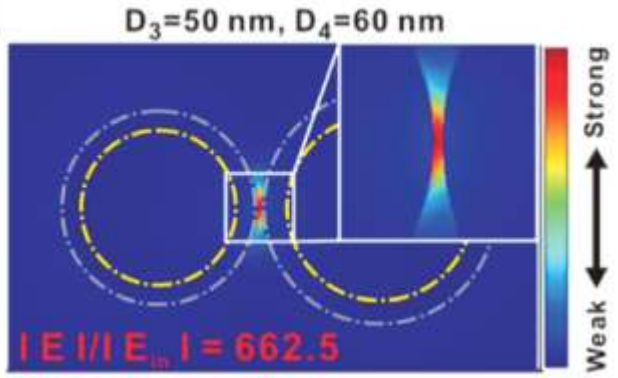

Nam J. M. et al. Plasmonic nanogap-enhanced Raman scattering with nanoparticles //Accounts of chemical research. – 2016. – Т. 49. – №. 12. – С. 2746-2755.

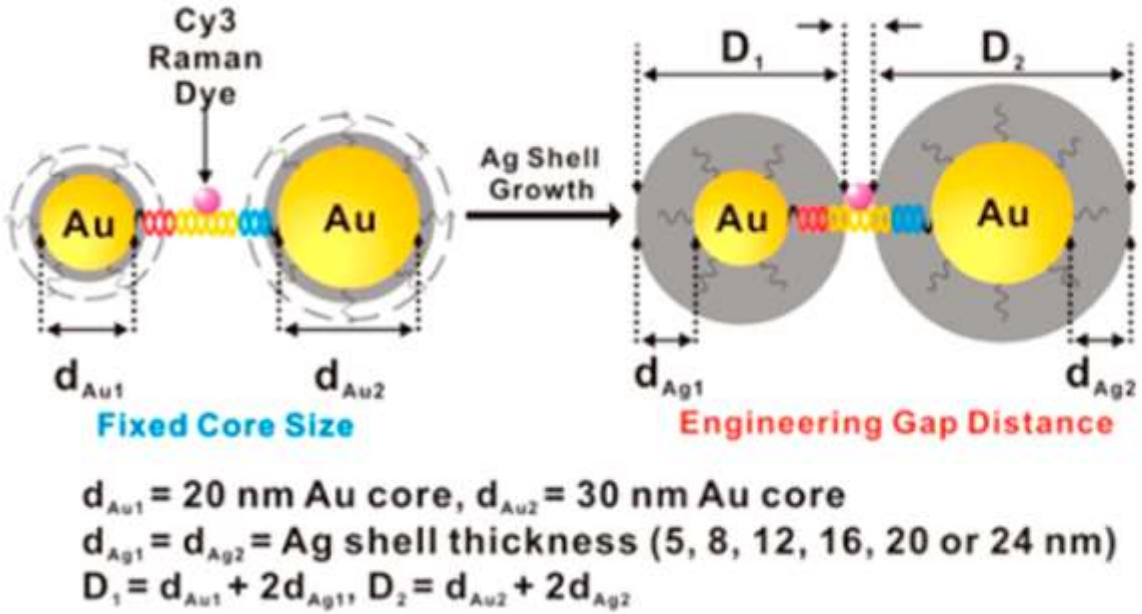

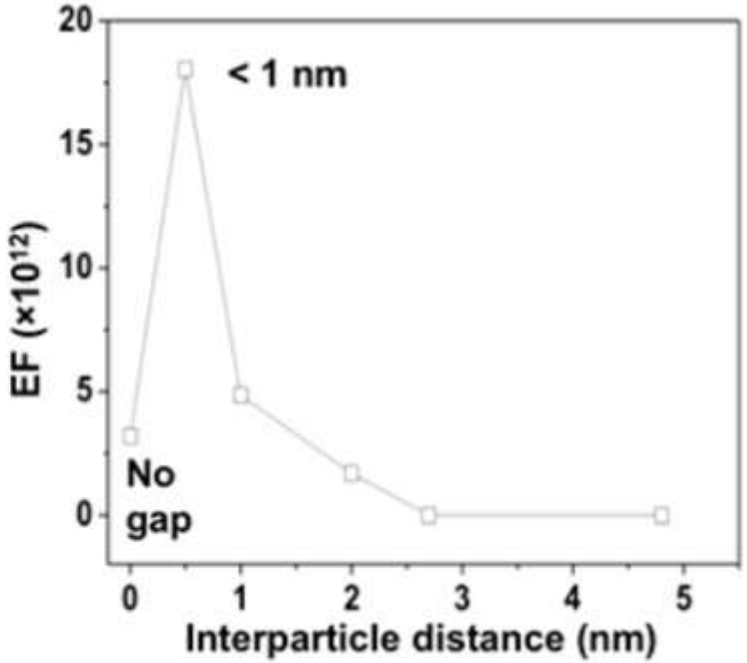

Surface-Enhanced Raman Scattering from Large Gold Nanoparticle Arrays

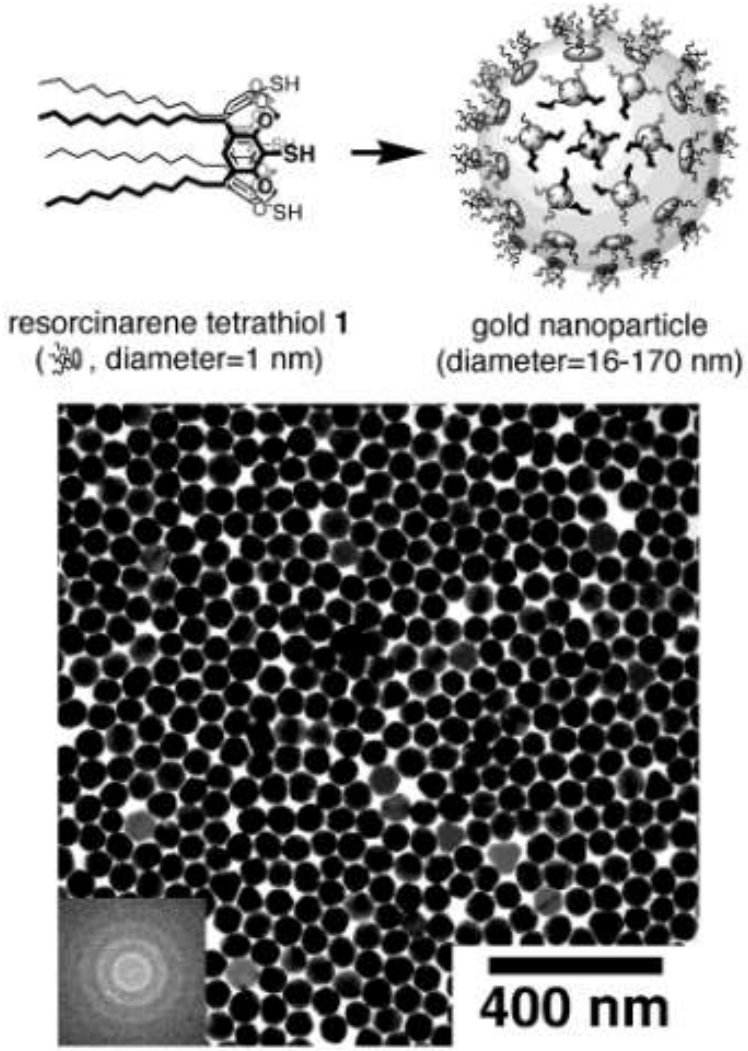

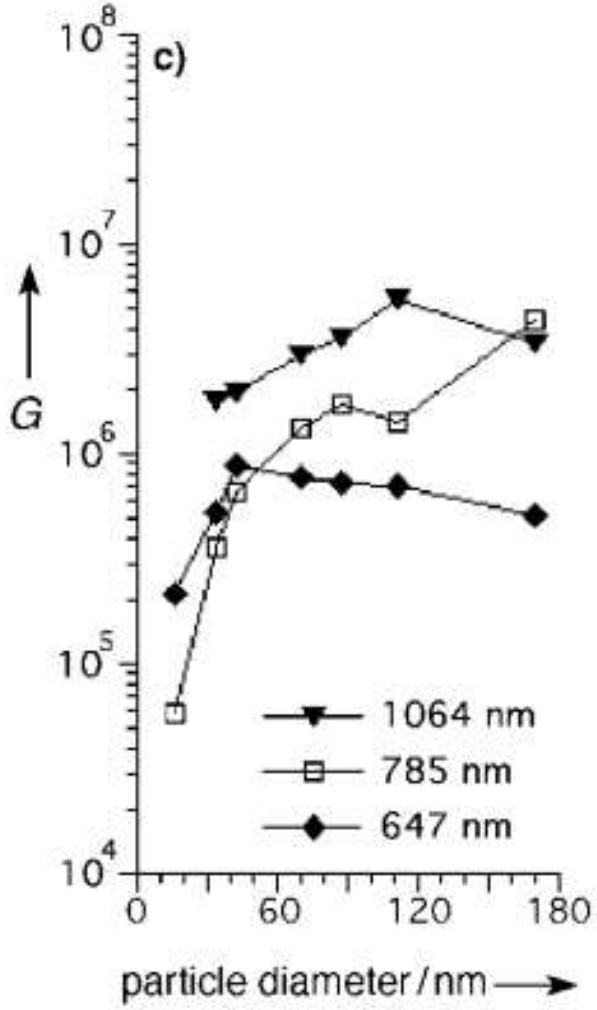

Kim B., Tripp S. L., Wei A. Self-organization of large gold nanoparticle arrays //Journal of the American Chemical Society. – 2001. – Т. 123. – №. 32. – С. 7955-7956.

Wei A. et al. Tunable surface-enhanced Raman scattering from large gold nanoparticle arrays //ChemPhysChem. – 2001. – Т. 2. – №. 12. – С. 743-745.

Tip-enhanced Raman spectroscopy (TERS)

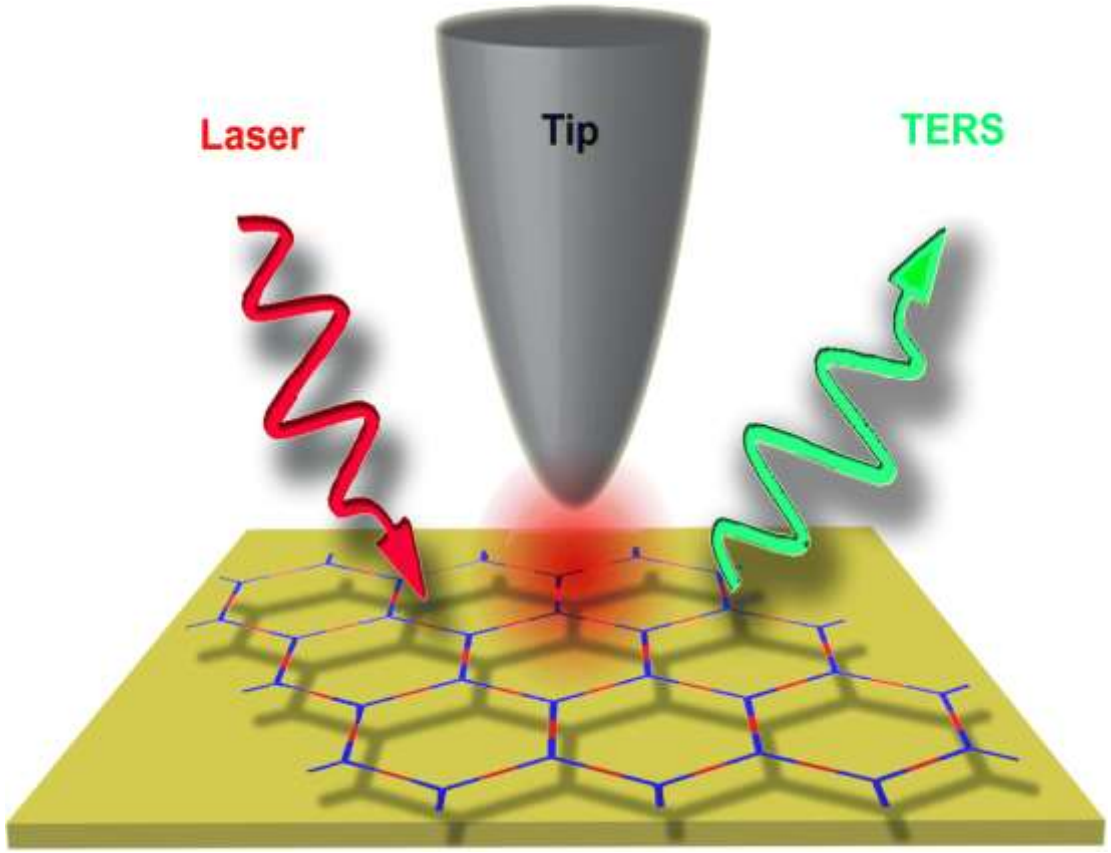

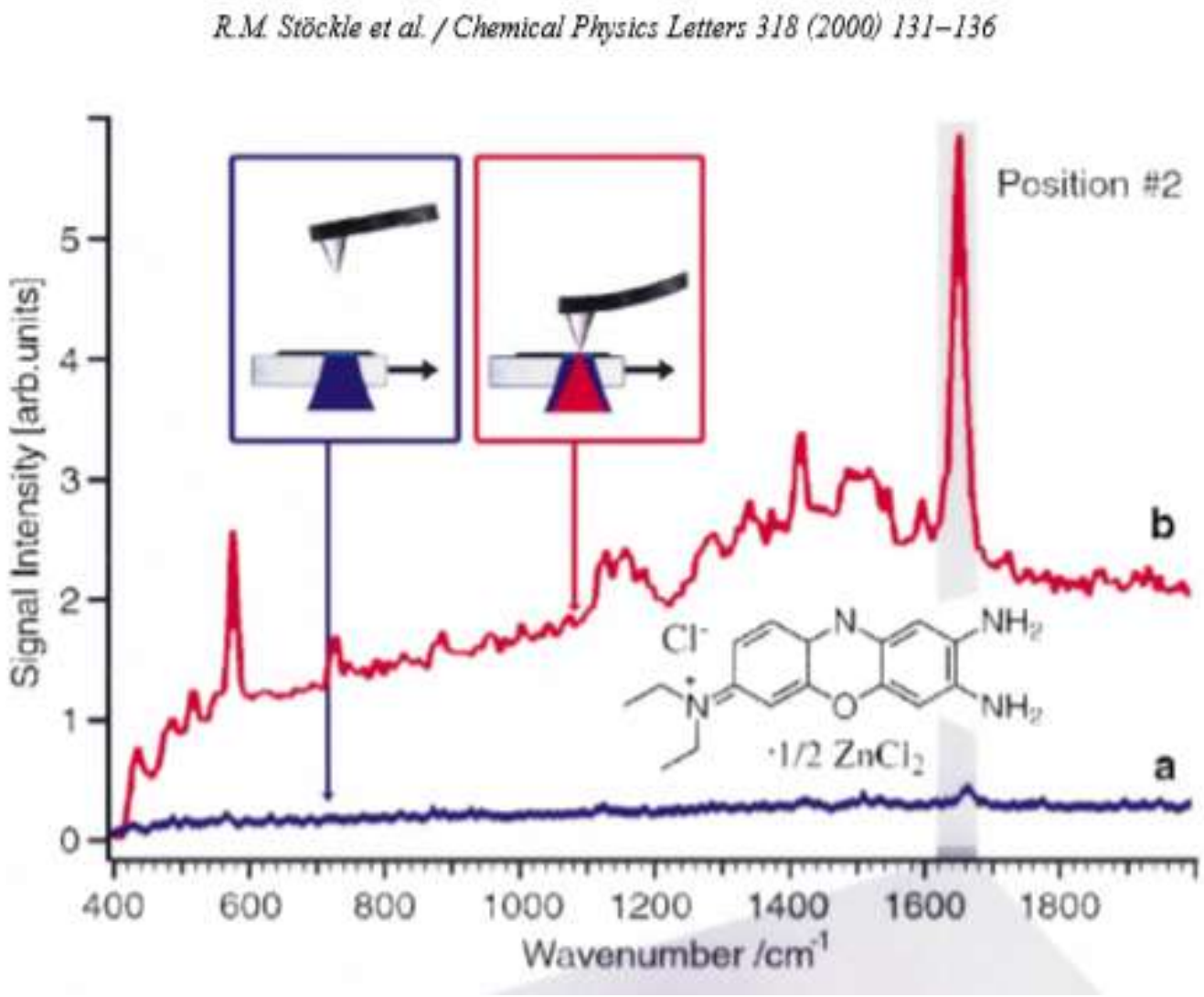

AFM images of Ag thin films with different rms roughness, ranging from 0.83 nm to 7.14 nm.

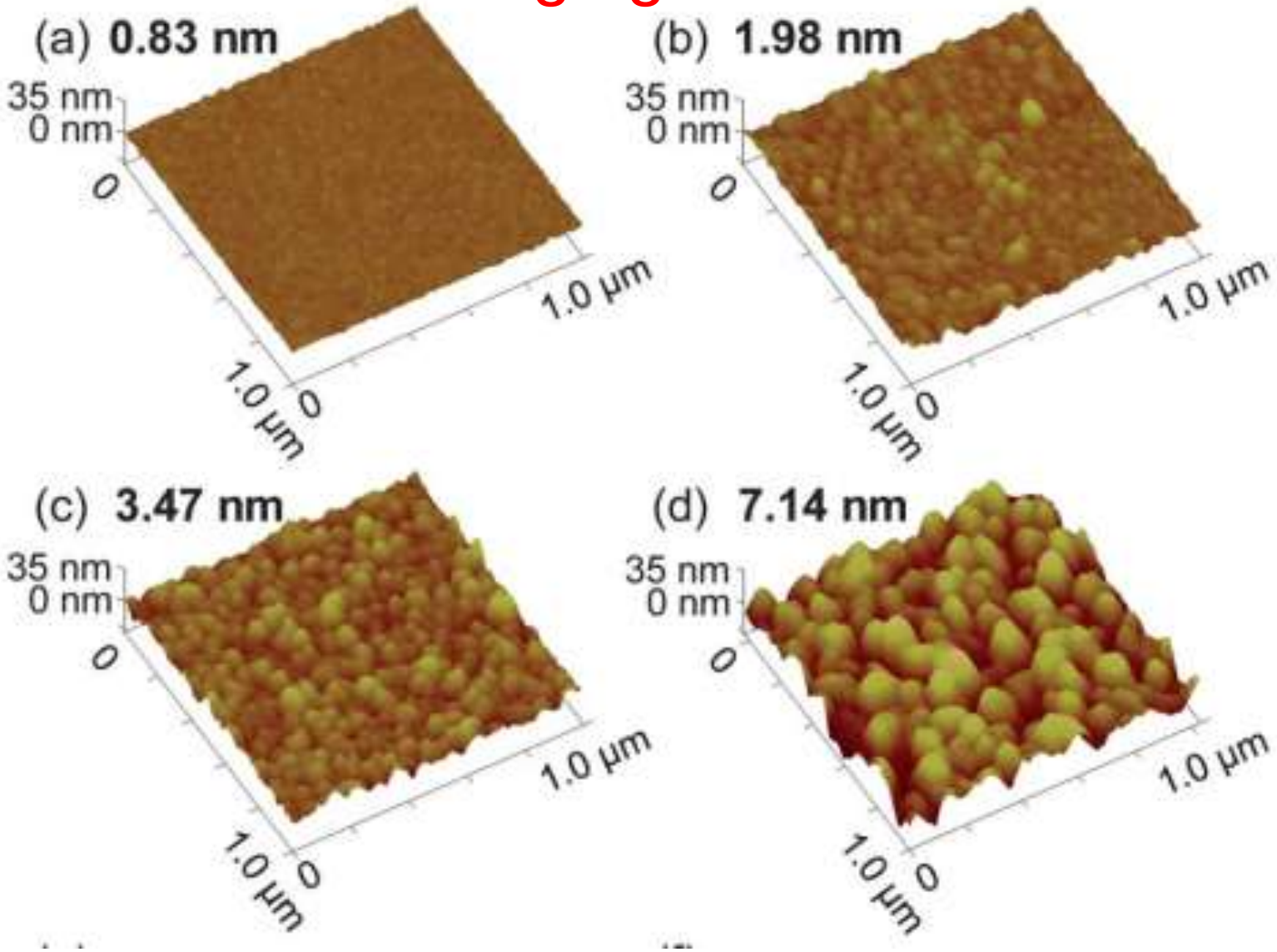

The smoothest film, was deposited by thermal evaporation. Ag thin films with larger roughness were deposited by sputtering at different deposition rates (1, 0.67 and 0.33 nm/s). The thickness of Ag thin films to be around 100 nm

Zhao Y. et al. Effects of surface roughness of Ag thin films on surface-enhanced Raman spectroscopy of graphene: spatial nonlocality and physisorption strain //Nanoscale. – 2014. – Т. 6. – №. 3. – С. 1311-1317.

Raman spectra of graphene on rough Ag thin films and the Si substrate

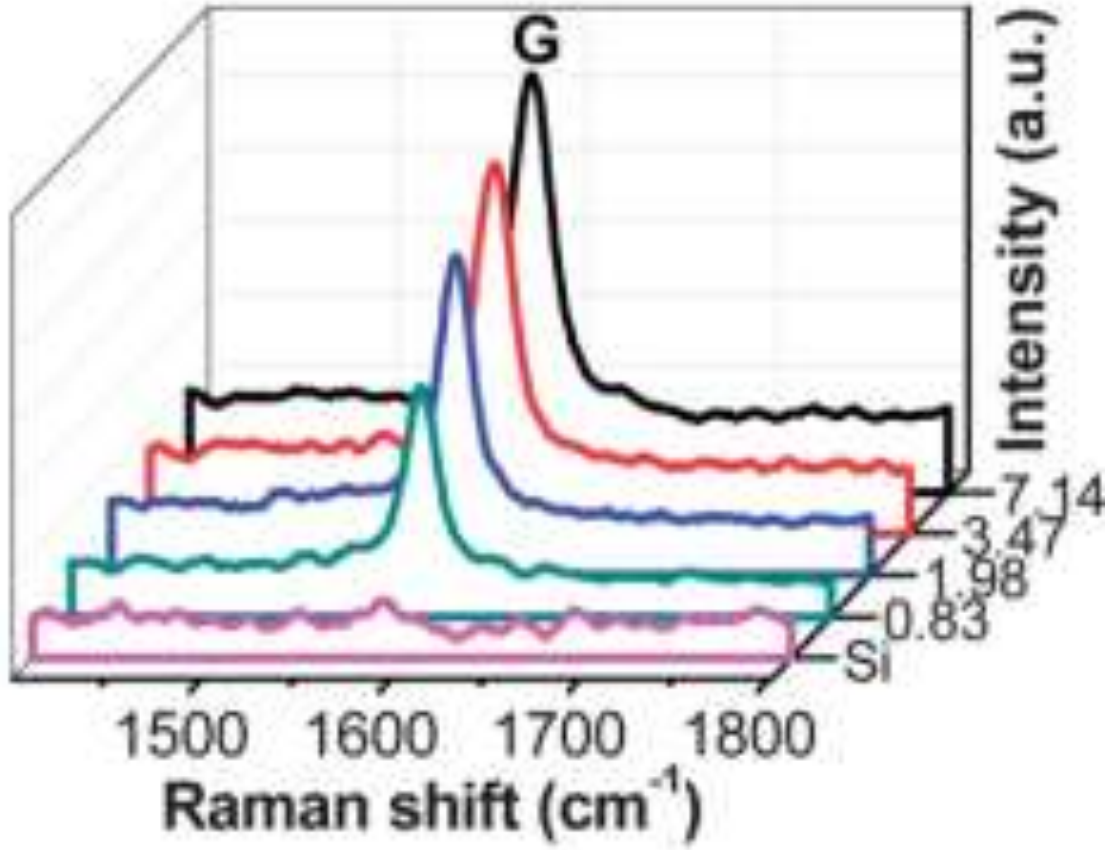

The enhancement factor of Raman intensity on Ag films with different roughness compared with that on the Si substrate

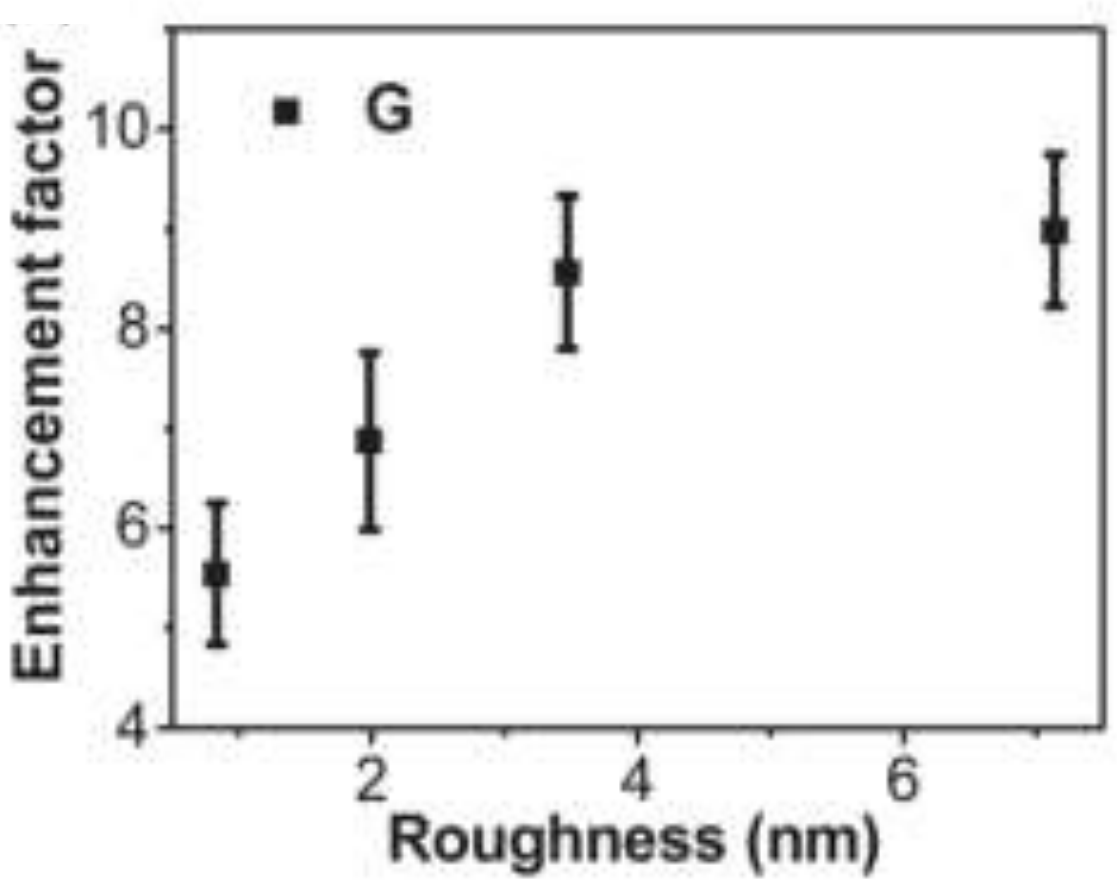

Raman spectroscopy (HORIBA HR800) with the excitation wavelength of 488 nm was used. A 100x objective was used to focus the laser beam and to collect the Raman signal. The size of the laser spot is about 1 mm.

Surface-Enhanced Raman Scattering

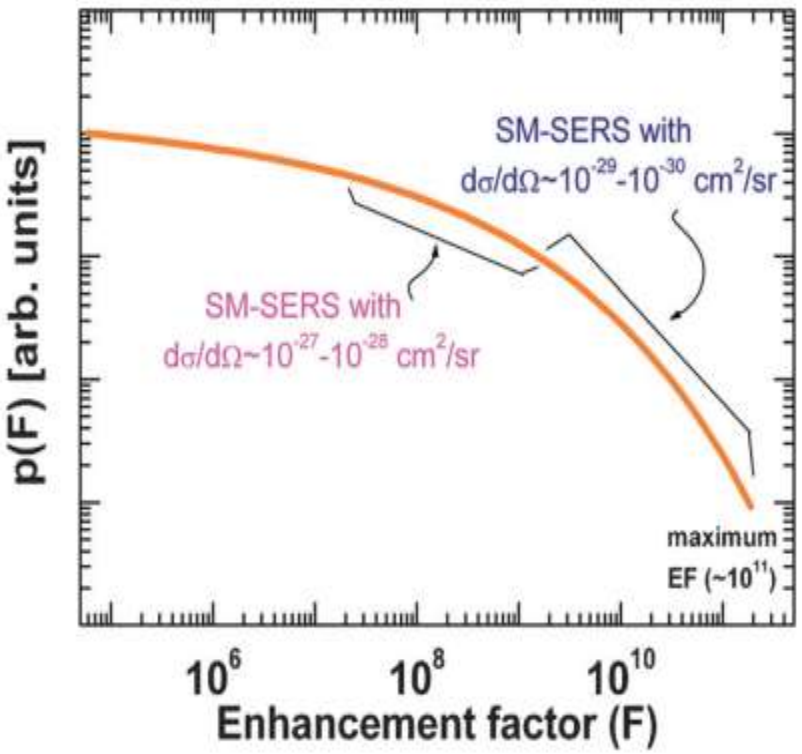

Figure 3. Long-tail probability distribution of enhancement factors (EFs) in SERS. From Ref. [29].

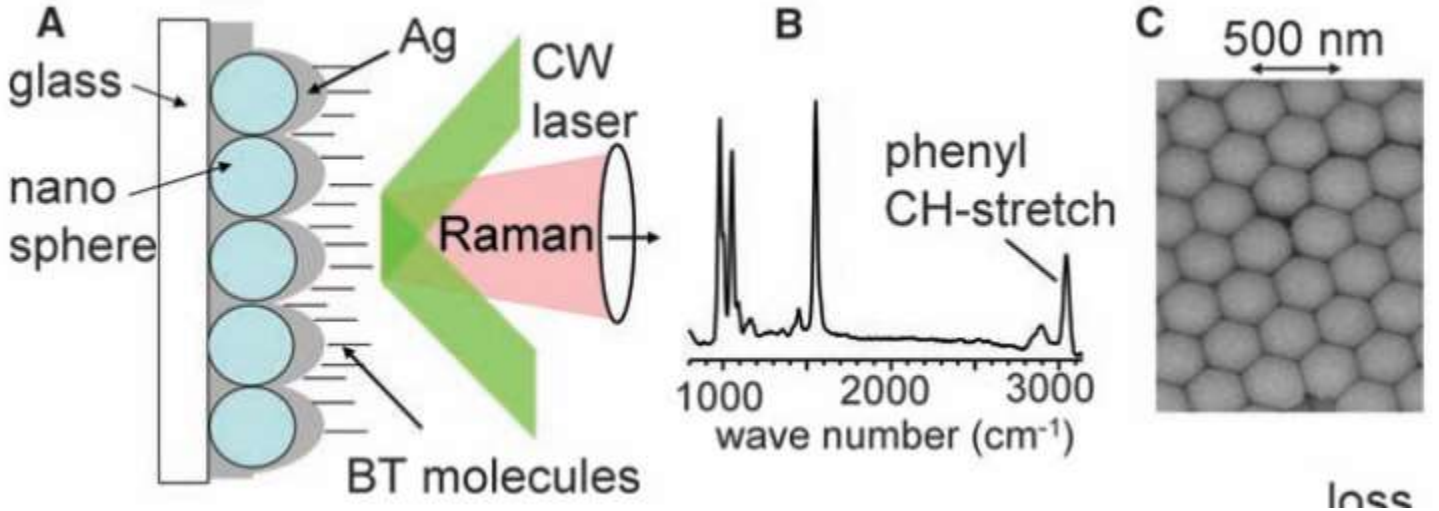

Raman enhancement factor η	Percentage of molecules	Percentage contribution to overall SERS signal
$<2.8 \times 10^4$	0	0
2.8×10^4 to 1×10^5	61%	4%
10^5 to 10^6	33%	11%
10^6 to 10^7	5.1%	16%
10^7 to 10^8	0.7%	22%
10^8 to 10^9	0.08%	23%
10^9 to 10^{10}	0.006%	17%
$>10^{10}$	0.0003%	7%

Fang Y., Seong N. H., Dlott D. D. Measurement of the distribution of site enhancements in surface-enhanced Raman scattering //Science. – 2008. – Т. 321. – №. 5887. – С. 388-392.

Single Molecule Detection Using Surface-Enhanced Raman Scattering (SERS)

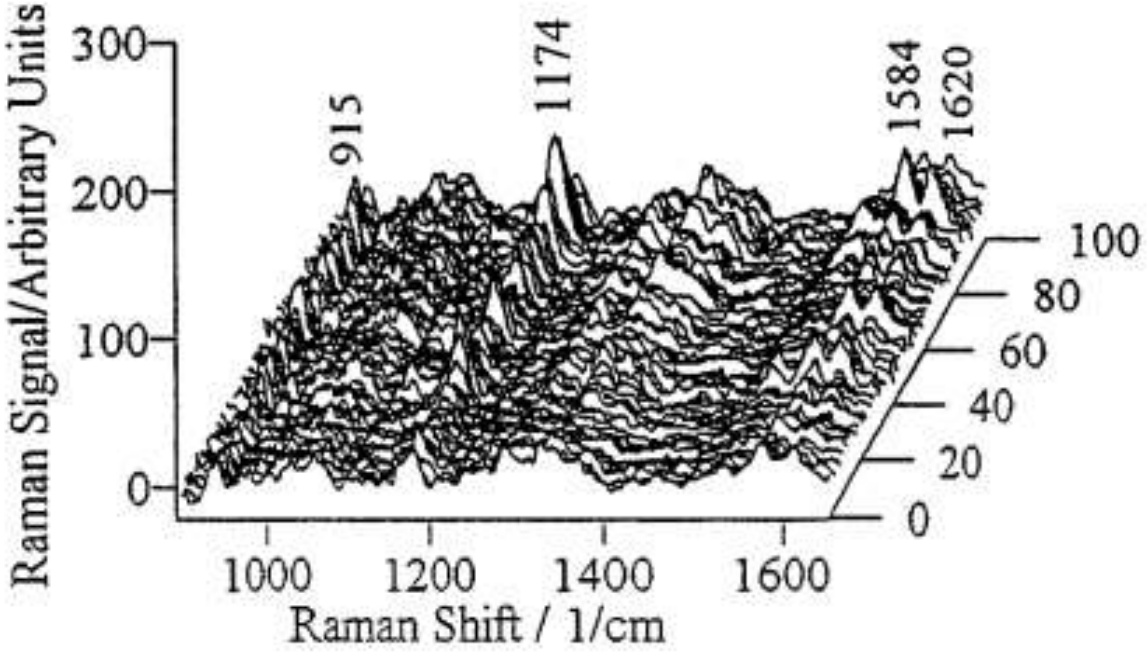

SERS spectra collected from a 30 pl scattering volume containing an average of 0.6 crystal violet molecules

Crystal violet
(Трифенилметан)

cw Ti:sapphire laser operating at **830 nm (200 Mw).** Chromex spectrograph with a deep depletion CCD detector.
A water immersion microscope objective (x63, NA 0.9) was brought into direct contact with a 30 ml droplet of sample solution for both excitation and collection of the scattered light.
Scattering volume was estimated to be approximately 30 pl. An average of 0.6 molecules in the probed 30 pl volume

Kneipp K. et al. Single molecule detection using surface-enhanced Raman scattering (SERS) //Physical review letters. – 1997. – Т. 78. – №. 9. – С. 1667.

(a) Peak heights of the 1174 cm^{-1} line for the 100 SERS spectra shown in Fig. 1. (b) Signals measured at 1174 cm_{21} for 100 spectra from a sample without crystal violet to establish the background.

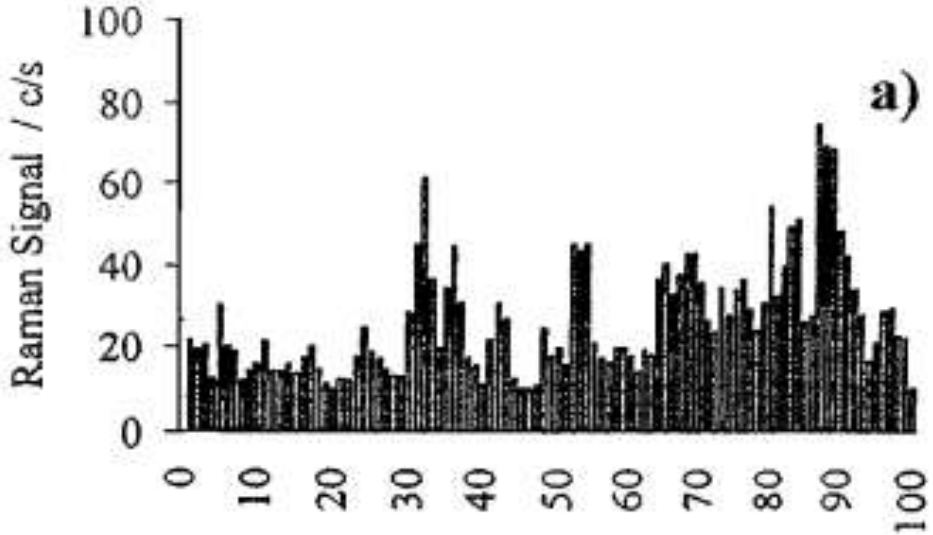

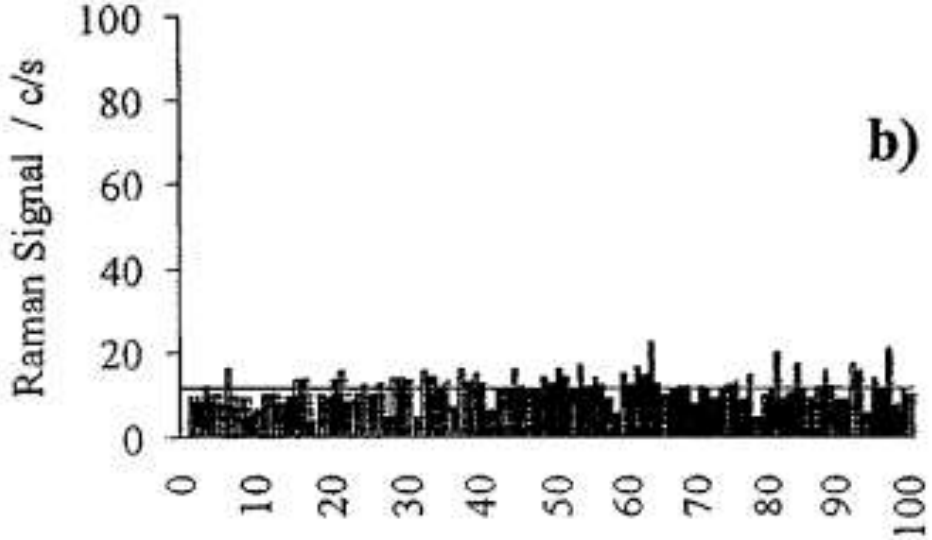

Statistical analysis of 100 SERS measurements (1174 cm_{21} Raman line) for an average of 0.6 crystal violet molecules in the probed volume. The peaks reflect the probability to find just 0, 1, 2, or 3 molecules in the scattering volume

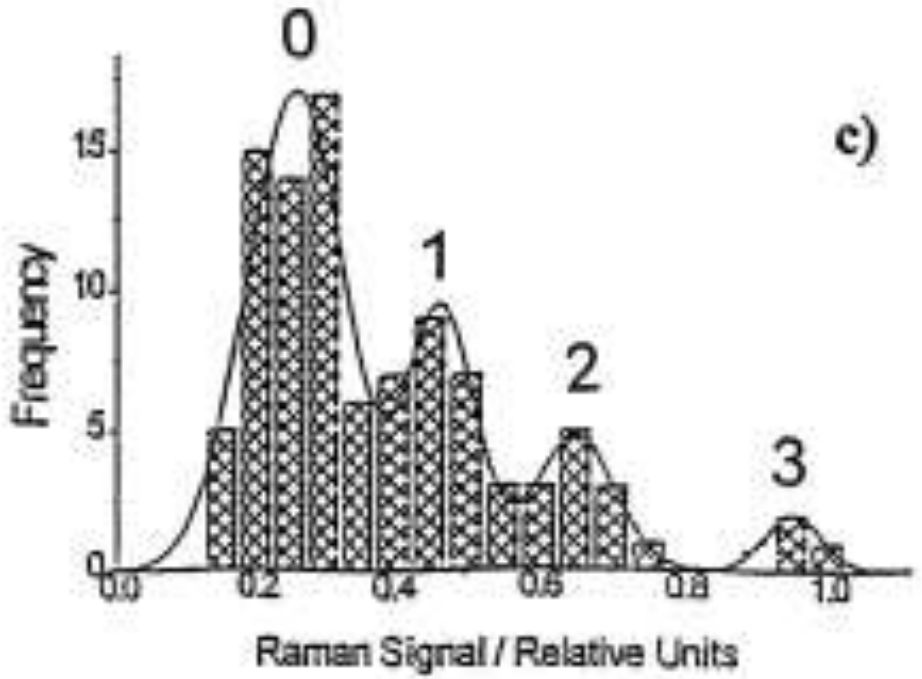

Raman scattering enhancement contributed from individual gold nanoparticles and interparticle coupling

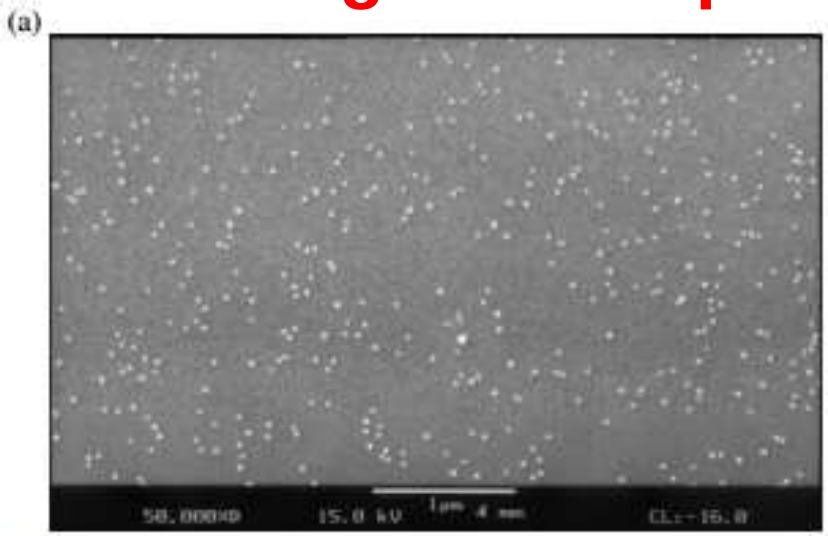

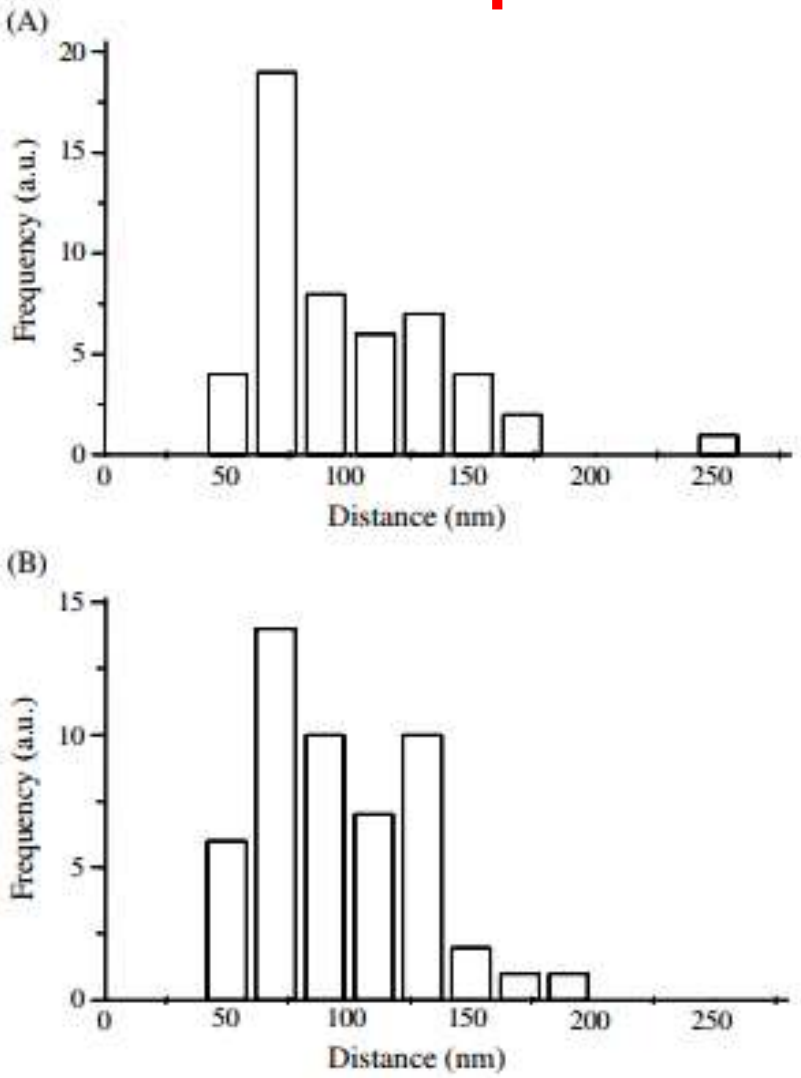

Zhu Z., Zhu T., Liu Z. Raman scattering enhancement contributed from individual gold nanoparticles and interparticle coupling //Nanotechnology. – 2004. – Т. 15. – №. 3. – С. 357.

The SEM images of the 22 nm colloidal gold assemblies on APS modified silicon wafers

(e)

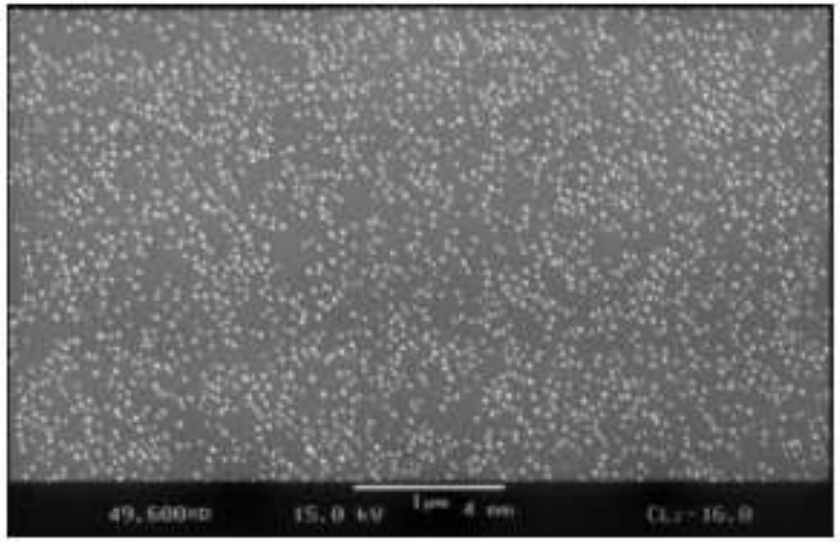

(E)

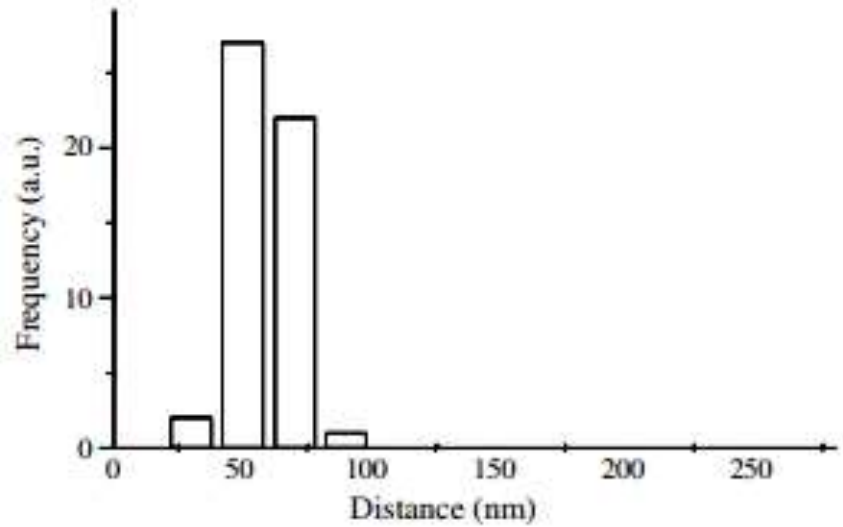
Frequency (a.u.)
0
10
20
0
50
100
150
200
250
Distance (nm)

(f)

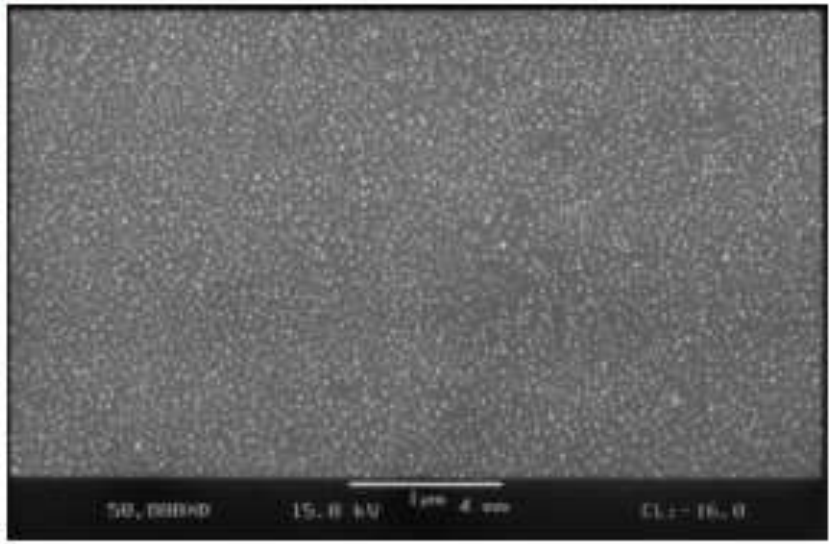

(F)

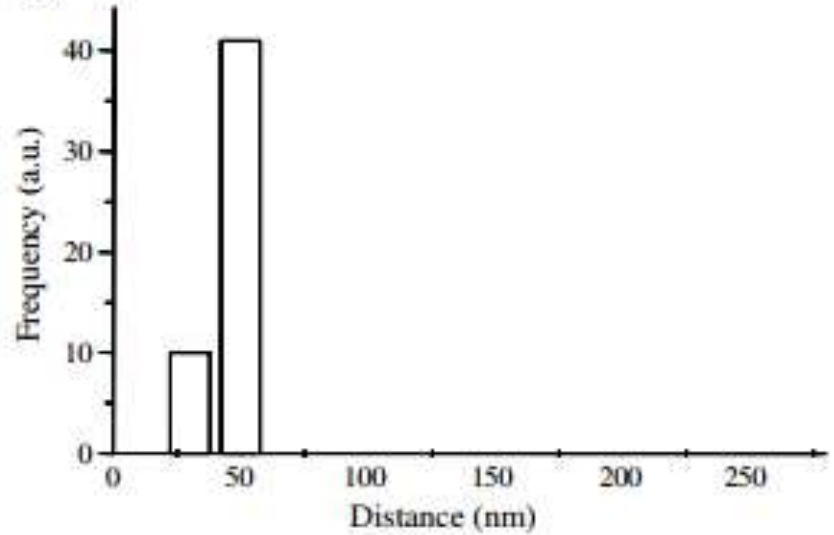
Frequency (a.u.)
0
10
20
30
40
0
50
100
150
200
250
Distance (nm)

The relationship between the enhancement factors and the average interparticle distances

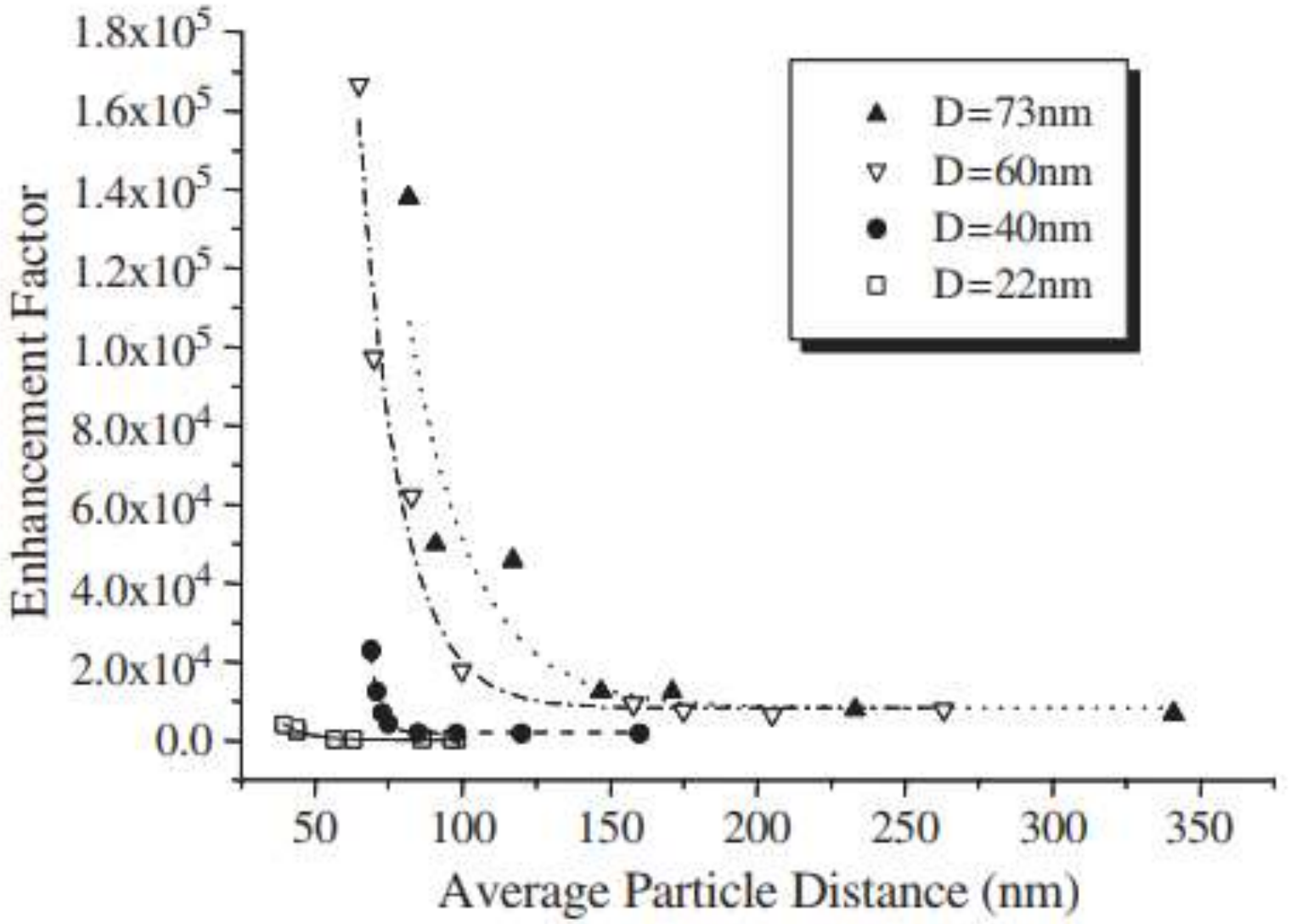

Nanostructures for SERS

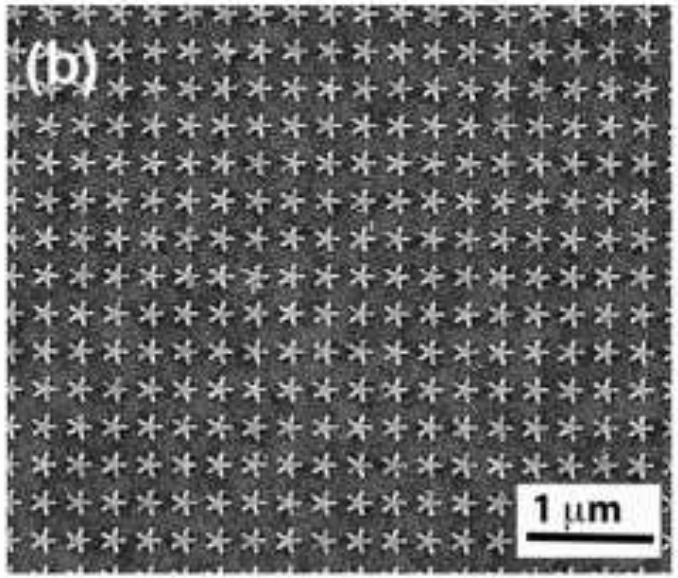

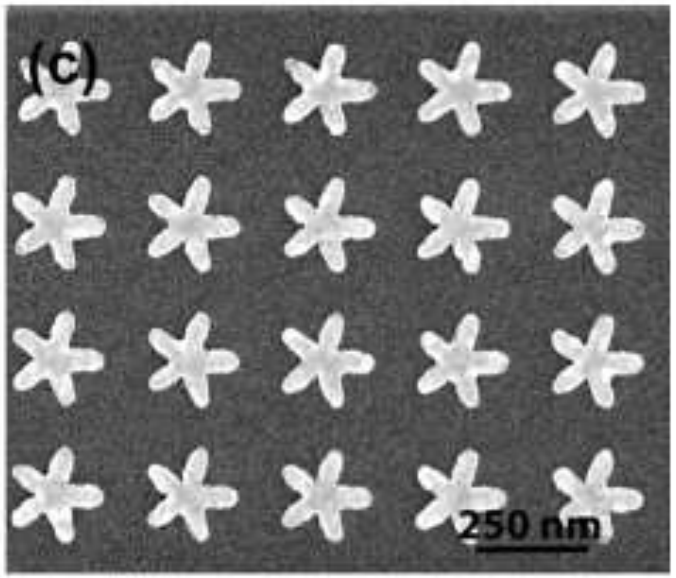

Enhancement ~ 10^4 Das G. et al. Plasmonic nanostars for SERS application //Microelectronic Engineering. – 2013. – T. 111. – C. 247-250.

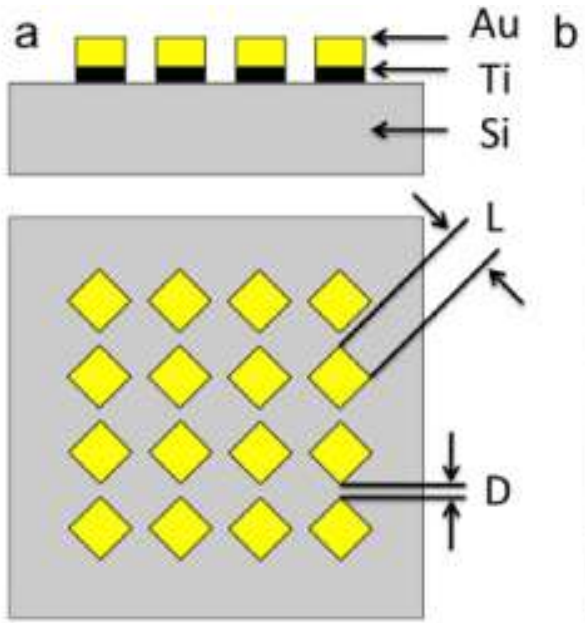

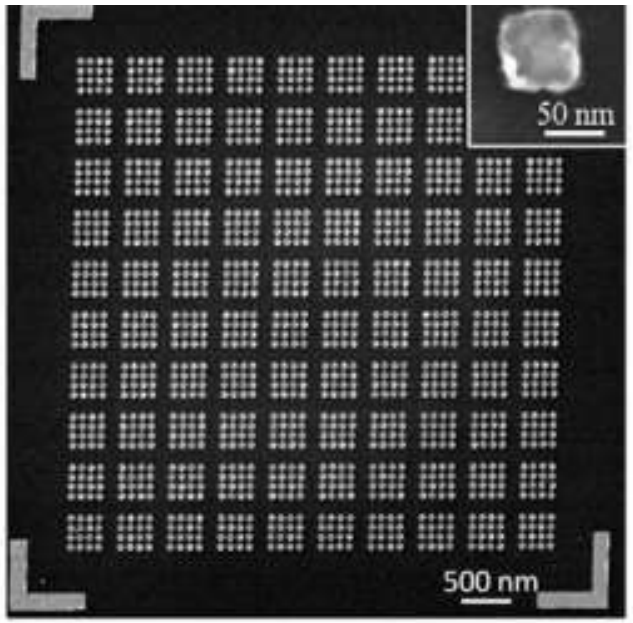

Enhancement ~ 10^4 Chirumamilla M. et al. Optimization and characterization of Au cuboid nanostructures as a SERS device for sensing applications //Microelectronic Engineering. – 2012. – T. 97. – C. 189-192.

“SERSitive”

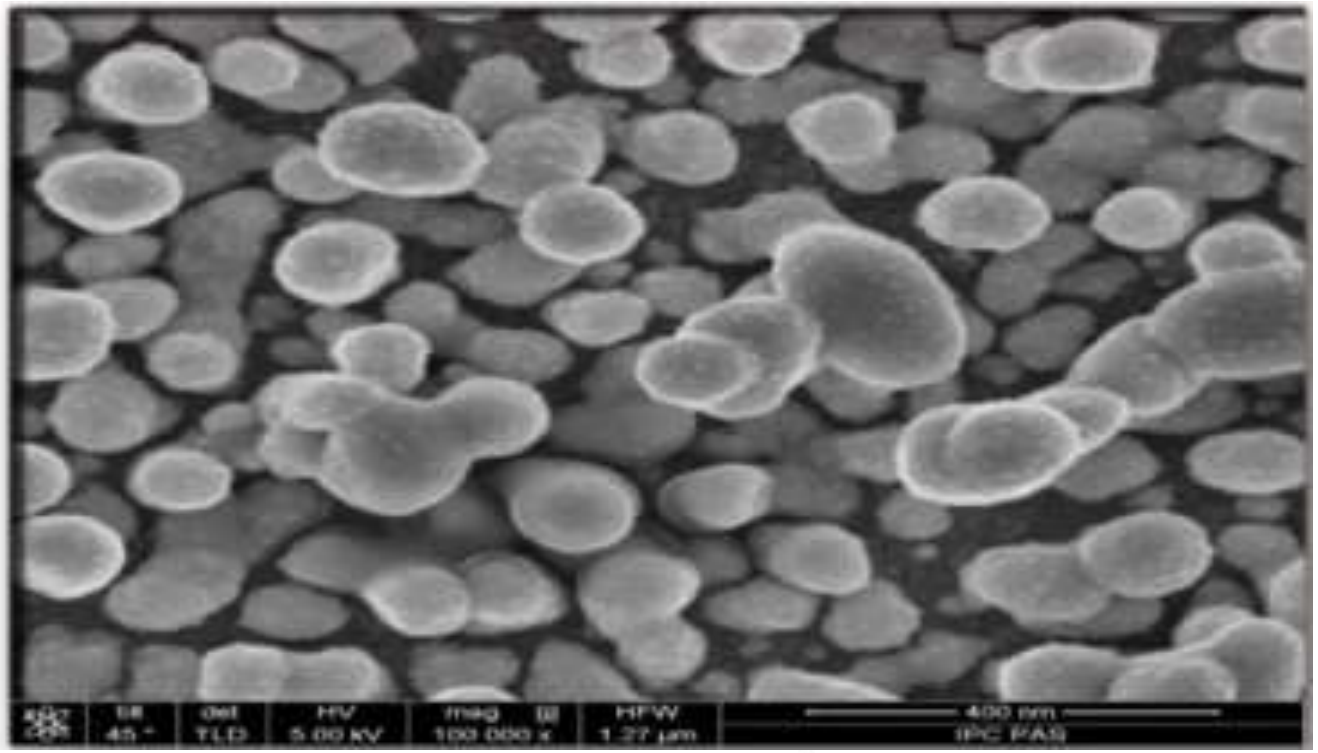

SERS substrates are prepared using ar electrodeposition of silver and gold nanoparticles on an ITO glass surface

€180.00 5 pcs

Feature	Value
Dimensions	9 x 7 x 0,7 mm *(width x height x thickness)*
SERS active surface	5 x 4 mm *(width x height)*
Active metal	Ag, Ag/Au hybrids
Substrate material	ITO glass
Sampling methods	drop deposition, immersion
Laser wavelength	514 nm, 633 nm, 785 nm *(recommended)*
Stability	up to 4 months
Ef	$10^5 - 10^6$

€350.00 5 pcs

Enhancement > 10^8

SILMECO

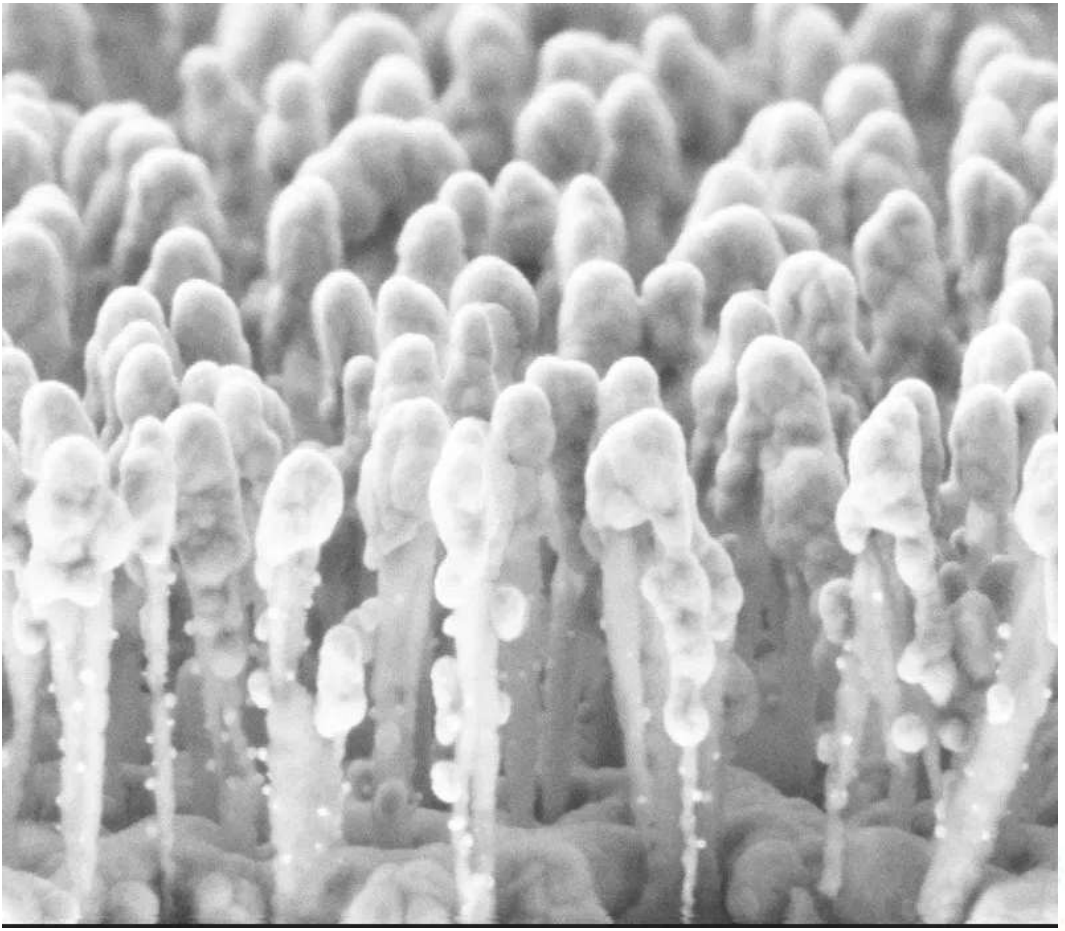

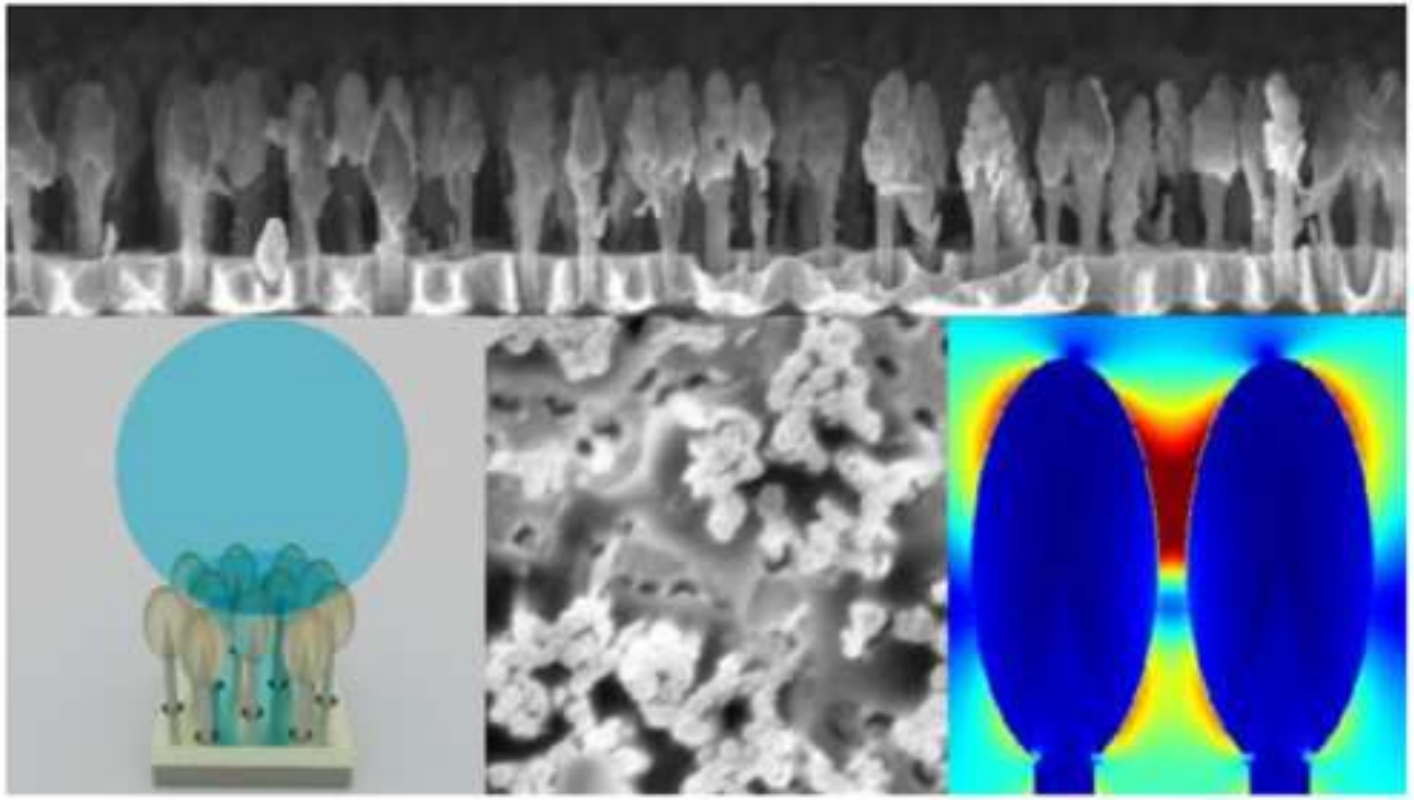

Fig. 1. Profile SEM image of the Ag nanopillar SERS substrates (top). The pillars are roughly 400 nm in height. Schematic picture of the structure with a droplet and water capillaries (left). SEM image of nanoparticle clusters that have been pulled together by the elasto-capillarity (middle). Cartoon demonstrating how the electromagnetic fields around two pulled together nanopillars can look like (right).

Hakonen A. et al. Detecting forensic substances using commercially available SERS substrates and handheld Raman spectrometers //Talanta. – 2018. – Т. 189. – С. 649-652.

Ocean Optics

€68 pcs

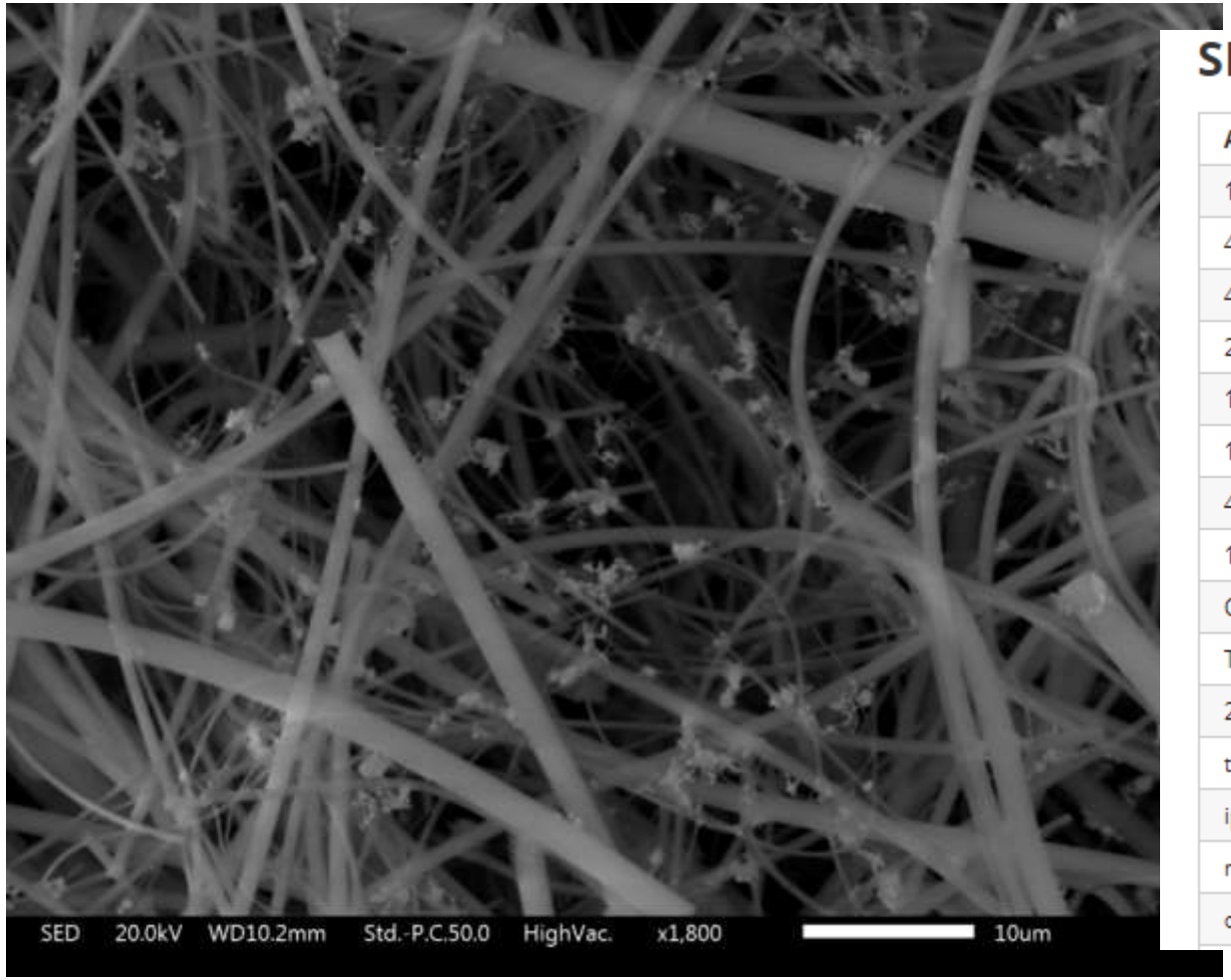

SERS Analytes Library – Limits of Detection

Analyte	Classification
1,2-bis(4-pyridyl)ethylene (BPE)	Taggant / Marker
4-mercaptobenzoic acid	Taggant / Marker
4-mercaptopyridine	Taggant / Marker
2-naphthalenethiol	Taggant / Marker
1,10-phenantroline	Taggant / Marker
1,2-Bis(4-pyridyl)ethane (BPYE)	Taggant / Marker
4,4'-Trimethylenedipyridine (TMDP)	Taggant / Marker
1,4-Diethynylbenzene (DEB)	Taggant / Marker
Cocaine	Illict drug
THC	Illict drug (Cannabis)
2-propranolol	Beta blocker
triamterene	Diuretic
ipratropium bromide	Bronchodilator
nicotinamide	B vitamin
crystal violet	Fungicide

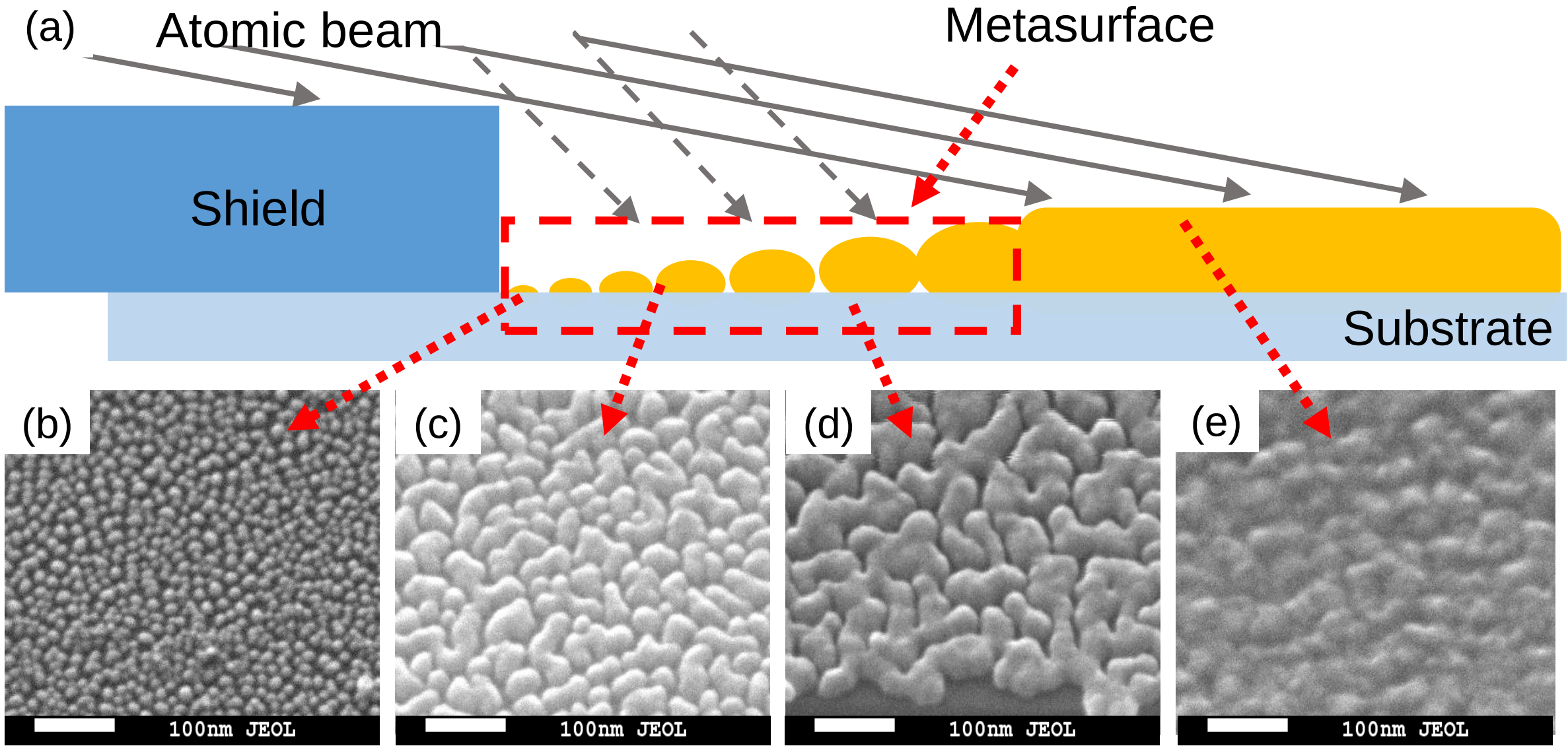
(a)
Atomic beam
Metasurface
Shield
Substrate
(b)
(c)
(d)
(e)
100nm JEOL
100nm JEOL
100nm JEOL
100nm JEOL

Клиновидная структура для SERS

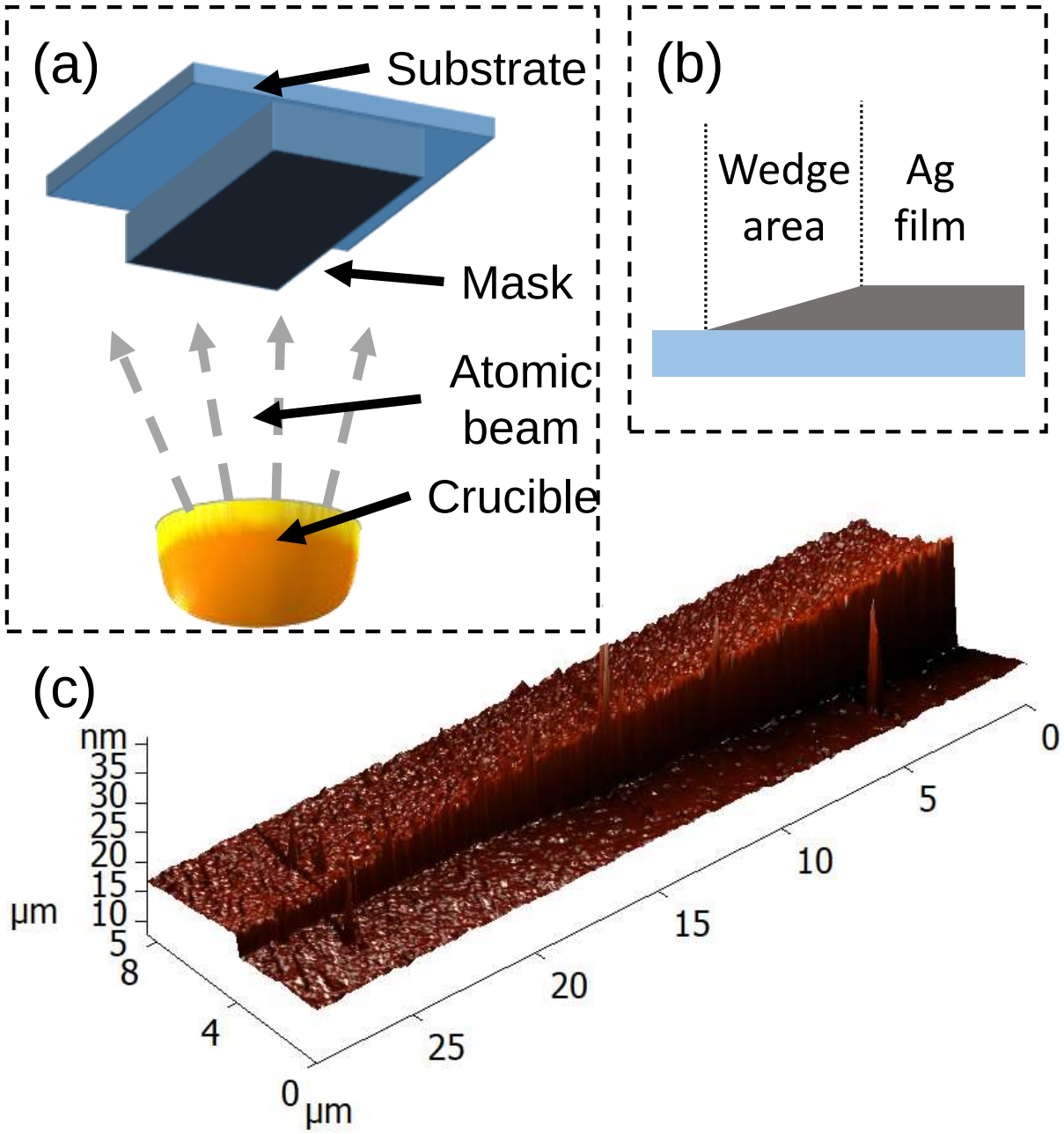

(a) Схема напыления клина: на подложке размещается маска, создающая область тени; (b) схема образца, можно выделить три области: сплошная пленка, область клина, чистая подложка; (c) AFM скан полученного клина

SEM клина

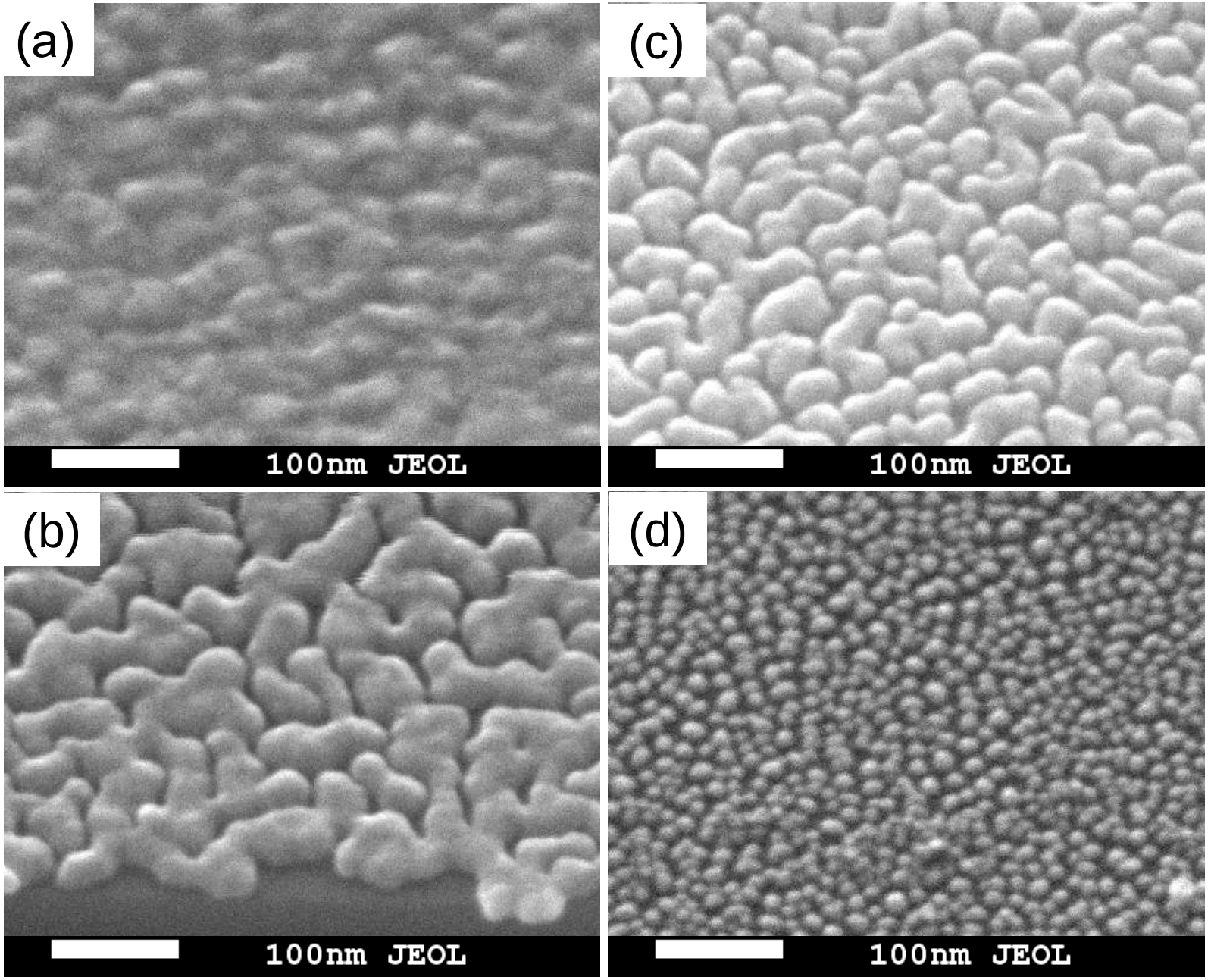

Изображение участков клина с разной толщиной полученной с покощью SEM: (a) толщина 60 нм, (b) толщина 30 нм, (c) толщина 15 нм, (d) толщина 4 нм

(a) Изображение клина «на просвет» в спектральной области пропускания фильтра FB780-10; (b) Усиление люминесценция Cy-7.5 в PMMA матрице на клине, возбуждение на длине волны 780 нм

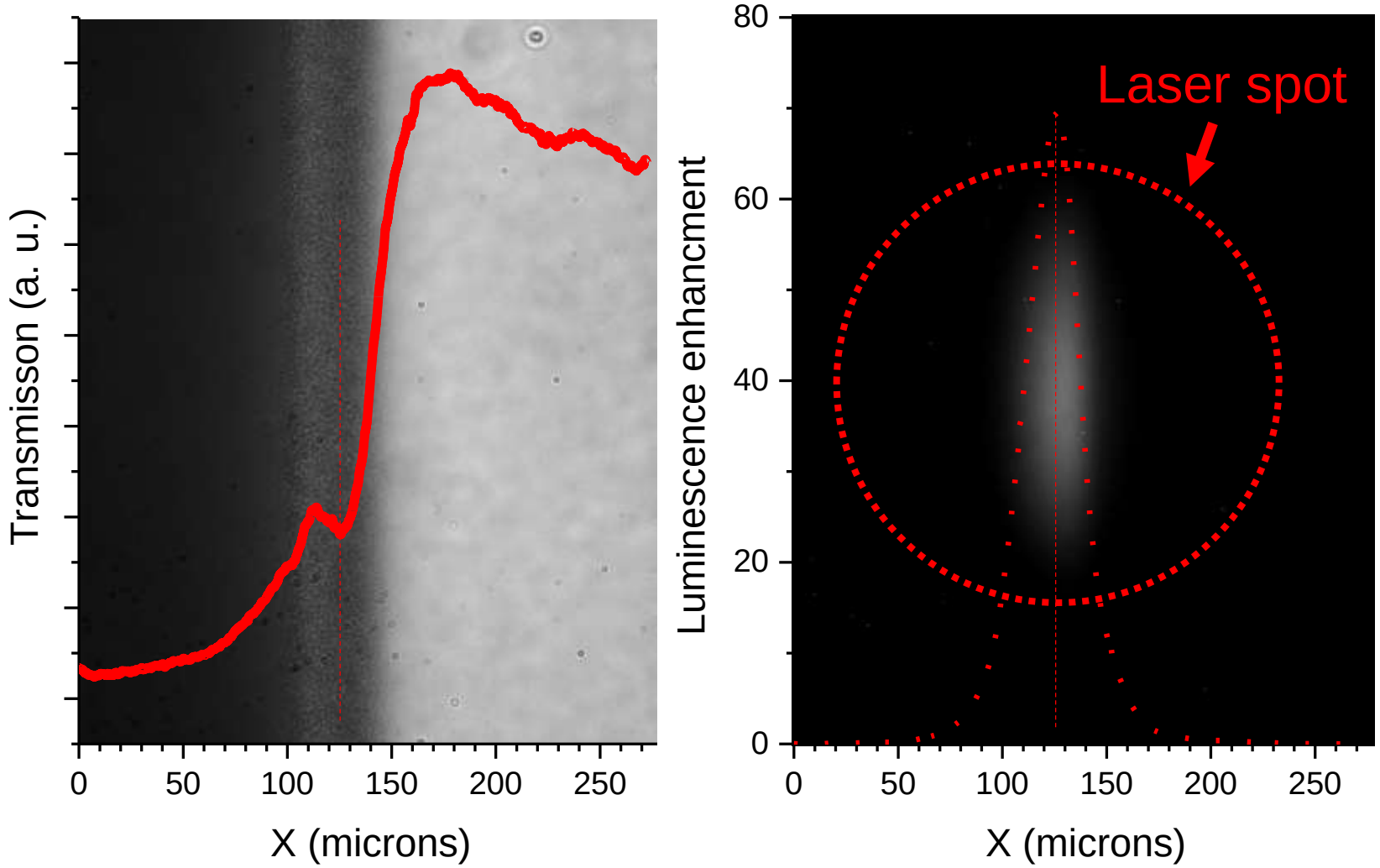

(a) Изображение клина «на просвет» при облучении коллимированным пучком света с центральной длиной волны 600 нм, спектральная ширина 40 нм, графиком показано изменение толщины образца; (b) срез изображение клина «на просвет» по оси X на разных длинах волн, видны характерные провалы, обусловленные плазмонным резонансом.

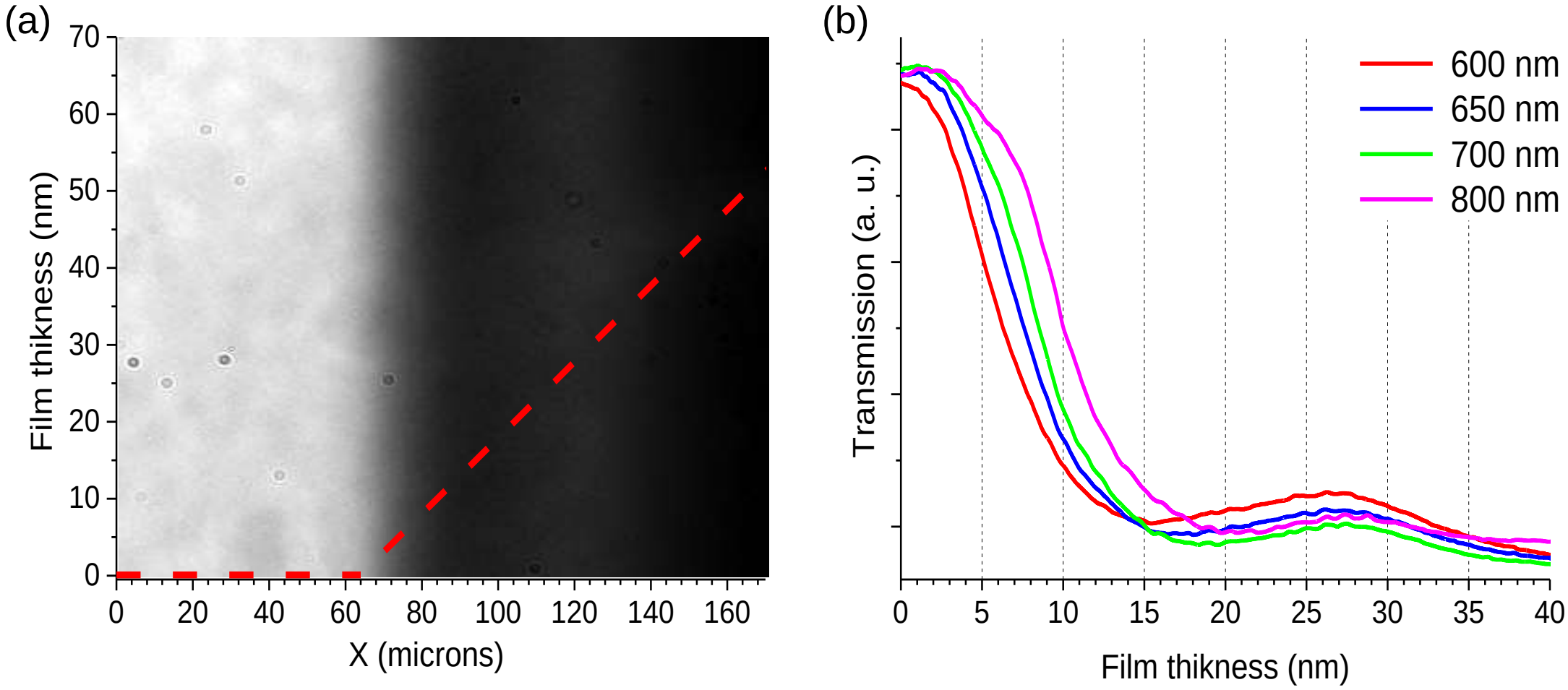

Зависимость толщины перкаляционной пленки от длины волны плазмонного резонанса

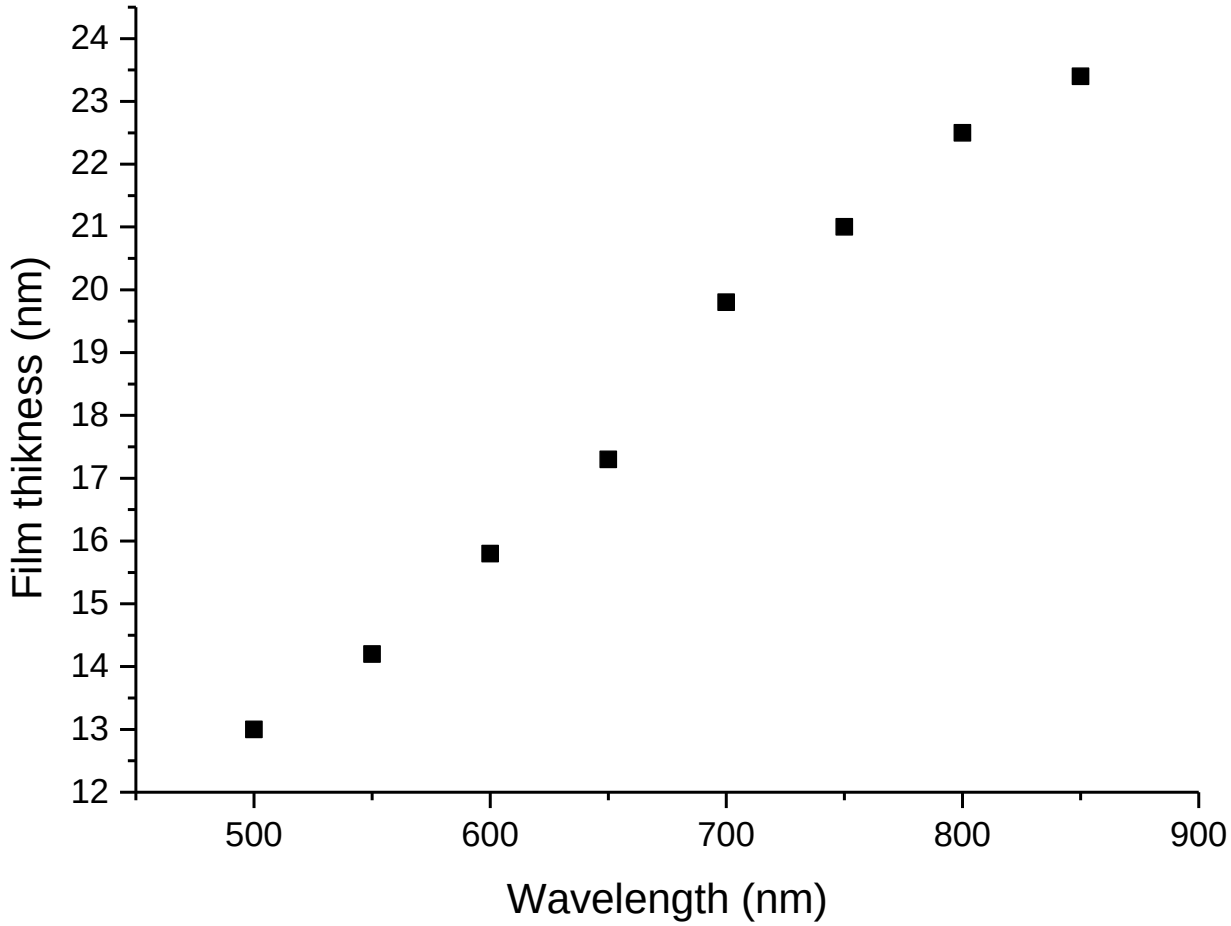

SERS benzene

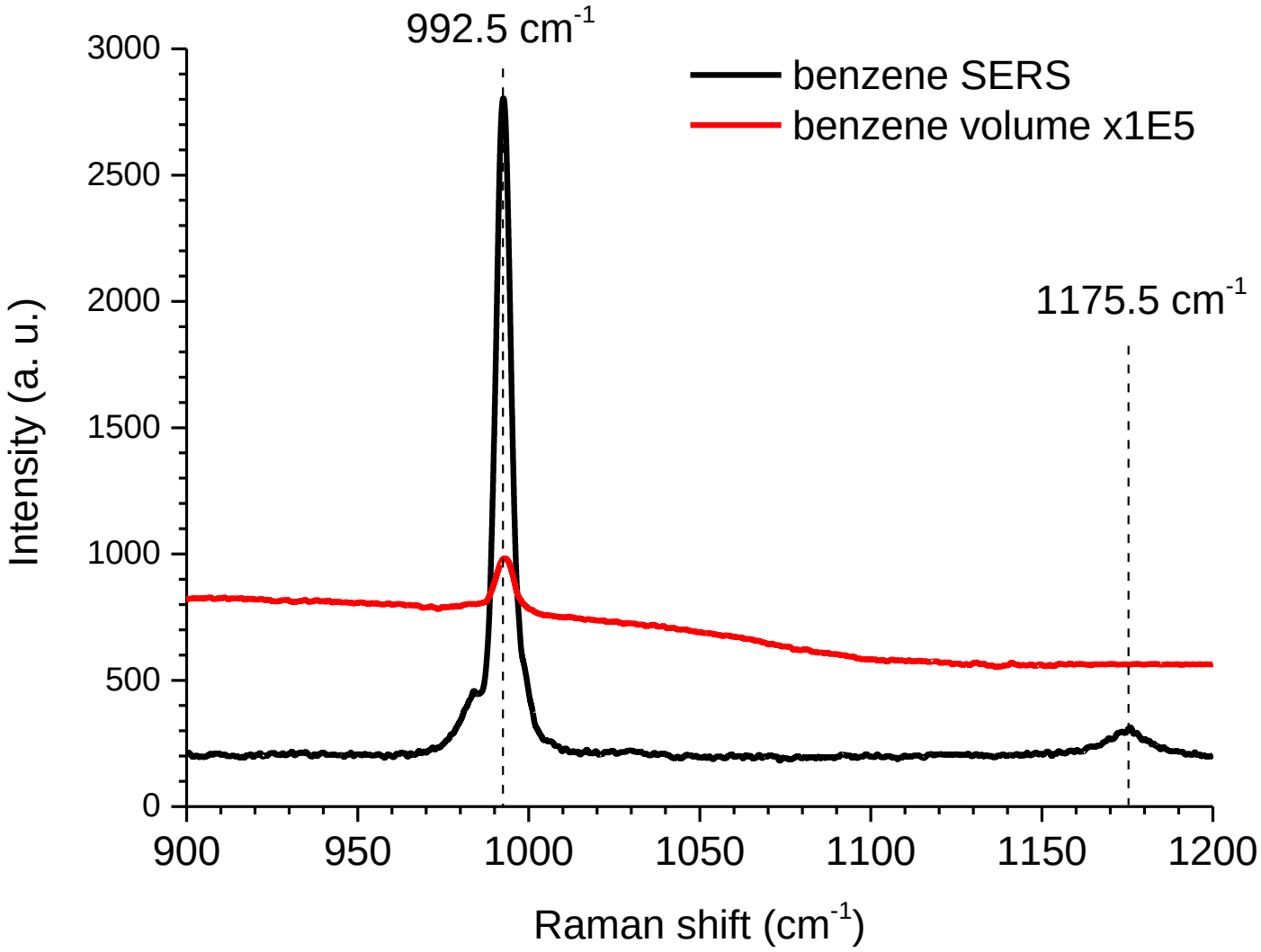

SERS Alq3

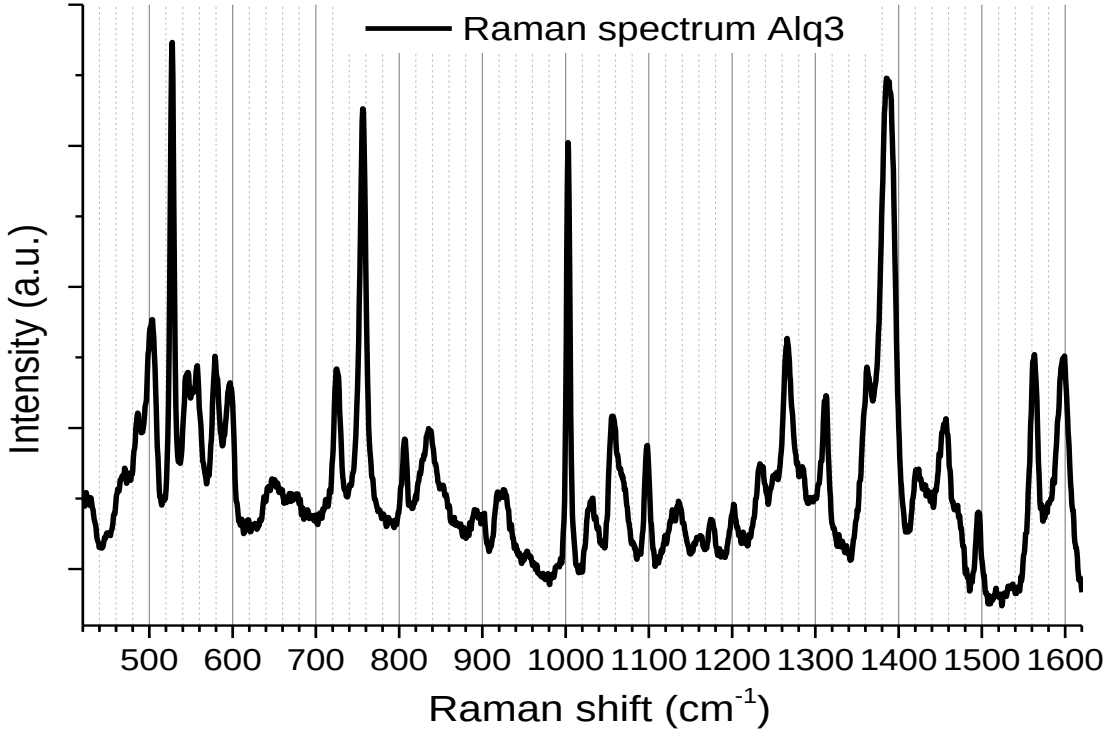

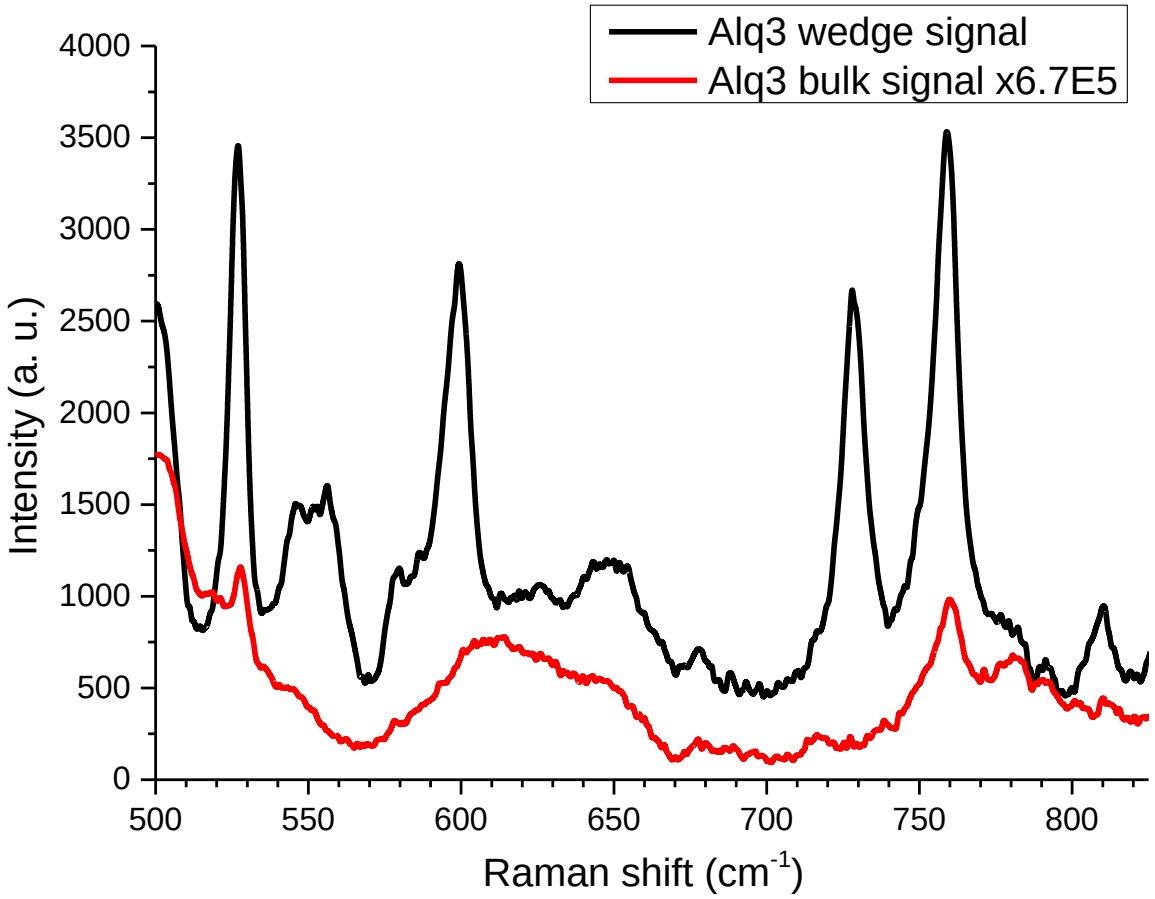

SERS enhancement factor 4E6